Sedimentary Geology 431 (2022) 106104

Contents lists available at ScienceDirect

Sedimentary Geology

journal homepage: www.elsevier.com/locate/sedgeo

Isotope composition ($\delta^{34}S$, $\delta^{18}O$) of the Middle Triassic-Early Jurassic sulfates in eastern Iberia

F. Ortí [a], A. Pérez-López [b,c,*], F. Pérez-Valera [d], C. Benedicto [e]

[a] Departament de Mineralogia, Petrologia i Geologia aplicada, Facultat de Ciències de la Terra, Universitat de Barcelona, (UB), C/ Martí Franquès s/n, 08028 Barcelona, Spain
[b] Departamento de Estratigrafía y Paleontología, Facultad de Ciencias, Avda. Fuentenueva, 18071 Granada, Spain
[c] Instituto Andaluz de Ciencias de la Tierra (CSIC-Universidad de Granada), Avda. de las Palmeras, 4, 18100 Armilla, Granada, Spain
[d] Dpto. de Ciencias de la Tierra y del Medio Ambiente, Facultad de Ciencias, Universidad de Alicante, Carr. de San Vicente del Raspeig, s/n, 03690 San Vicente del Raspeig, Alicante, Spain
[e] Ilustre Colegio Oficial de Geólogos (ICOG) 7557, C/ El Castillo 83 bajo, 12429 El Toro, Castelló de la Plana, Spain

ARTICLE INFO

Article history:
Received 10 December 2021
Received in revised form 3 February 2022
Accepted 13 February 2022
Available online 18 February 2022

Editor: Dr. Catherine Chagué

Keywords:
Evaporites
isotopy
Triassic
Keuper
Muschelkalk
Iberia

ABSTRACT

This study combines published isotope data (223 samples) with new data (153 samples) on the $\delta^{34}S$ and $\delta^{18}O$ composition of Ca-sulfate rocks (anhydrite and secondary gypsum) accumulated in eastern Iberia during the Middle Triassic to Early Jurassic. The $\delta^{34}S$ mean values of the evaporite units reveal the following trends: a decrease from the lower Anisian (~18‰) to the Carnian-Norian interval (~15‰); an increase at the Rhaetian (~16‰); a decrease in the Hettangian-Sinemurian interval (~14‰); and finally an increasing trend from the Sinemurian-Pliensbachian (~16‰) to the Pliensbachian-Toarcian (~19‰). This $\delta^{34}S$ isotope assemblage together with the generalized low standard deviations observed for the different evaporite units is consistent, and suggests that the isotope composition of these Ca-sulfates are primary signatures related to feeding marine water sulfate. Depending on the evaporite units, these $\delta^{34}S$ mean values are, nevertheless, ~1‰ to ~3‰ lower than those reported for coeval Triassic evaporites of the Germanic basin and the Alp-Apennine domains. In eastern Iberia, the $\delta^{18}O$ values are more variable and also display wider scatters than the corresponding $\delta^{34}S$ values. Of particular interest in our study are: (i) the low $\delta^{34}S$ values for the Anisian in comparison with those in the Germanic basin; (ii) the shift to heavier values in the Rhaetian, recorded for first time in the evaporites of eastern Iberia; (iii) the low values observed for the Hettangian, which suggest that the change to the heavier values of the Jurassic (~19‰) occurred after the end-Hettangian in eastern Iberia; and (iv) the affinity of the $\delta^{34}S$ values recorded for the Hettangian-Sinemurian interval to those known for the Canadian domain.

1. Introduction

Sulfate (SO_4^{2-}) is a major component of marine water, and different processes have modified its $\delta^{34}S$ and $\delta^{18}O$ isotope composition in the ocean throughout the Earth's history. Initial attempts to establish global age curves of variation in $\delta^{34}S$ and $\delta^{18}O$ in marine sulfate evaporites during geological periods were done by Holser and Kaplan (1966), Holser (1977), Claypool et al. (1980) and Lindh (1983), among others. Since then, some of these curves have significantly improved, particularly the sulfur isotope curves (Strauss, 1997; Kampschulte and Strauss, 2004; Bernasconi et al., 2017). The most direct source of documentation has been the isotope analysis of Ca-sulfate precipitates (gypsum and anhydrite) in evaporite formations whose marine origin is firmly established. Additionally, sulfur isotope values of structurally substituted sulfate (SSS; carbonate associated sulfate, CAS) have been obtained in the calcite lattice of sedimentary carbonates (Newton et al., 2004; Prokoph et al., 2008; Song et al., 2014; Schobben et al., 2015; He et al., 2020).

In many sedimentary basins, however, the isotope composition of sulfur and oxygen ($\delta^{34}S$, $\delta^{18}O$) of sulfate evaporites has been poorly characterized leading to a lack of precision in the isotope age curves on global scales. Similarly, this lack of accurate isotope determinations may prevent the correct discrimination between a marine or non-marine origin of the evaporite formations, especially when their Ca-sulfate facies are similar or the original successions have been disrupted by severe tectonism or diapirism.

The Iberian microplate, in the westernmost area of the Tethys Sea, is one of the geological domains in which the difficulties mentioned above affect the very rich evaporites record of Triassic age accumulated during the initial stages of the Pangea break-up (Gordon, 1975; Warren, 2006). In 'eastern Iberia', i.e. the eastern part of the Iberian Massif currently dominated by Mesozoic and Cenozoic sedimentary rocks (Fig. 1A), the thickest and most varied record of Mesozoic evaporites corresponds to the Middle Triassic-Early Jurassic time interval (Ortí et al., 2017). Subsequently, these evaporites controlled firstly the structuration of Jurassic-

* Corresponding author at: Departamento de Estratigrafía y Paleontología, Facultad de Ciencias, Avda. Fuentenueva, 18071 Granada, Spain.
E-mail addresses: f.orti@ub.edu (F. Ortí), aperezl@ugr.es (A. Pérez-López), fperez@ua.es (F. Pérez-Valera), conbb2@gmail.com (C. Benedicto).

https://doi.org/10.1016/j.sedgeo.2022.106104
0037-0738/

Cretaceous sedimentary basins under an extensional regime, and secondly their Cenozoic deformation (Martínez del Olmo et al., 2015; Nebot and Guimerà, 2016; Flinch and Soto, 2017). As a result of this evolution, the Middle Triassic-to-Early Jurassic evaporites underwent significant chemical recycling, and the new precipitates derived from this recycling filled the non-marine depocenters of many Paleogene-Neogene basins (Utrilla et al., 1992).

The first aim of this paper is to provide isotope data ($\delta^{34}S_{VCDT}$, $\delta^{18}O_{VSMOW}$) for the Middle Triassic-Early Jurassic evaporites of eastern Iberia. These isotope data are analyzed by evaporite units, basins and

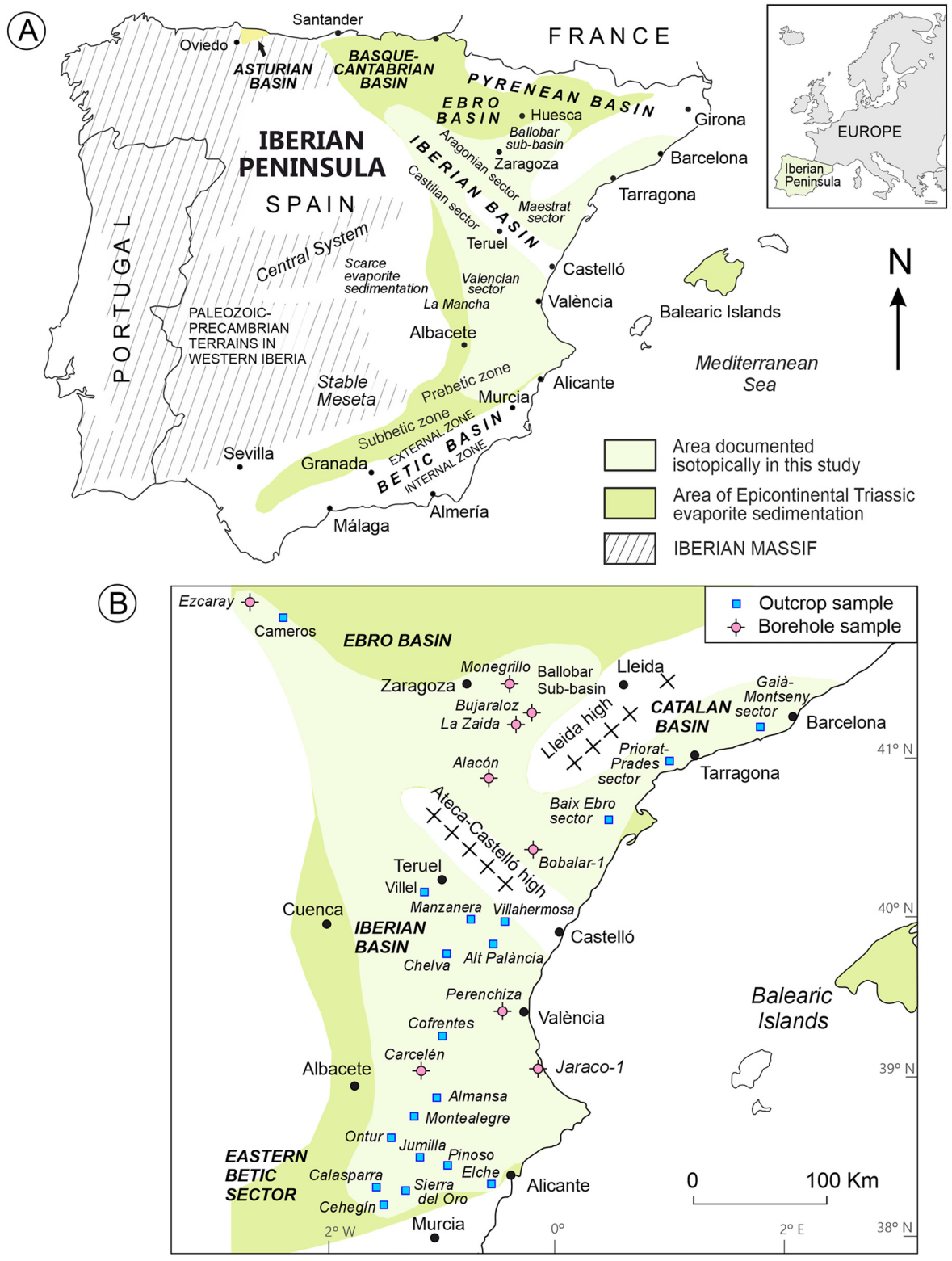

Fig. 1. Triassic basins, basin sectors and outcrops in eastern Iberia. (A) Geographic distribution of areas with preferent evaporite sedimentation of the Epicontinental Triassic. (B) Distribution of sampling sites and boreholes reported in this study. Symbols: Lines of crosses, paleohighs; open circles with cross, deep (oil) boreholes; Squares, outcrops/sections.

basin sectors, and their possible origins are discussed. Our sample dataset comes from an almost continuous sampling across the Triassic basins of eastern Iberia from the eastern sector of the Betic Cordillera in the south, to the Catalan Coastal Ranges and Ebro Valley in the north. A second aim is to compare our results with those known for the Triassic basins mainly in Central-Southern Europe (Germanic basin and Alp-Apennine domains) and in the Canadian domain in minor degree.

The evaporite record studied here extends from the early Anisian (Middle Triassic) to the Plienbachian-Toarcian (Early Jurassic). This study is particularly relevant for the Hettangian-Sinemurian given the scarcity of coeval evaporites in the Triassic basins of Central-Southern Europe. This feature contrasts with the abundance of these evaporites in North Atlantic areas during the Late Triassic-Early Jurassic (Holser et al., 1988). Our study will help improve present knowledge of isotope compositions of the Triassic and Early Jurassic evaporites of the western Tethys realm.

2. Geologic and stratigraphic setting

The break-up of the Pangea supercontinent and westwards migration of the Neotethys Ocean started at the end of the Permian (Ziegler, 1982, 1988). Late Permian-Early Triassic rifting resulted in the separation of a number of structural plates and microplates, one of which was Iberia (Preto et al., 2010; Stefani et al., 2010). The paleolatitude of Iberia during the Triassic and Early Jurassic, between 25° and 30 °N, was associated with long arid to semiarid periods of subtropical climate, although they were punctuated by some short episodes of moister climate (Gaetani et al., 2000; Thierry, 2000; Scotese et al., 2021). Several extensional systems interacted in eastern Iberia during the Late Permian-Early Triassic resulting in the creation of large depressions such as the Betic, Iberian, Catalan, Ebro, Pyrenean, Basque-Cantabrian, and Asturian basins (Arche and López-Gómez, 1996; Soto et al., 2017) (Fig. 1A). In most of these basins, sedimentary infill continued throughout the Mesozoic (Gibbons and Moreno, 2002; Vera, 2004).

Based on facies and paleogeography, the following Triassic types of lithostratigraphic successions are distinguished in eastern Iberia (Virgili et al., 1977; Sopeña et al., 1988; Gómez and Goy, 1998; López-Gómez et al., 1998): (i) the Hesperian Triassic type, including non-marine siliciclastics deposited at the eastern border of the emerged Iberian Massif (Fig. 1A); (ii) the Epicontinental (Germanic) Triassic type, deposited throughout eastern Iberia, with non-marine siliciclastics at the base (Buntsandstein facies), marine carbonates in the middle (Muschelkalk facies) and marine evaporites at the top (Keuper facies); (iii) and the Alpine Triassic type, in the south, mainly comprised of marine carbonates (allochthonous units of the Betic Internal Zone; Pérez-López and Pérez-Valera, 2007). In turn, the Muschelkalk facies of the Epicontinental (Germanic) Triassic consists of three units, i.e. carbonates of the lower Muschelkalk unit, siliciclastics and evaporites of the middle Muschelkalk unit, and carbonates of the upper Muschelkalk unit. This threefold arrangement of the Muschelkalk facies is known as the 'Mediterranean Triassic' and can be recognized from the Betic Cordillera in the southeast to the Catalan Coastal Ranges in the northeast.

Eastern Iberia preserves one of the best records of Triassic marine-derived evaporites in Europe (Escavy et al., 2012). This record is included within the following major stratigraphic units, they all becoming progressively wider from the Mediterranean coast towards the west (Ortí et al., 2017): Röt unit (early Anisian); middle Muschelkalk unit (middle-late Anisian); lower Keuper unit (latest Ladinian to early-middle Carnian); lower unit of the upper Keuper (late Carnian-early Norian); upper unit of the upper Keuper (Norian); and Anhydrite Zone (Rhaeto-Hettangian-Sinemurian). Besides, other Ca-sulfate horizons of less regional extension appear intercalated within the Middle Triassic and Early Jurassic carbonates in the eastern sector of the Betic basin and the Valencian sector of the Iberian basin (Fig. 1). These Ca-sulfate horizons occur in three carbonate successions: at the top of the upper Muschelkalk unit (at the uppermost part of the Royuela Formation; late Ladinian), towards the base of the Zamoranos Formation (Rhaetian), and within the Sinemurian-Toarcian interval (Fig. 2).

The Triassic basins and their paleogeographic sectors reported in this study are the following from south to north (Fig. 1A). *Betic basin*: eastern Betic sector (Subbetic and Prebetic zones of the Betic External Zone; Martín-Algarra and Vera, 2004); *Iberian basin*: Valencian and Maestrat sectors of the Castilian-Valencian Branch of the Iberian Ranges, and central sector of the Aragonian Branch of the same ranges; *Catalan basin*: Baix Ebre, Priorat-Prades, and Gaià-Montseny sectors; and *Ebro basin*: Ballobar sub-basin. The term 'Valencian sector' is used here in a broad sense and includes the whole València province, some adjacent areas of the Castelló, Teruel, Alicante and Cuenca provinces, and the eastern part of the La Mancha area (Albacete province).

The evaporite units of the Keuper facies were initially studied by Ortí (1974) in the Valencian sector of the Iberian basin. This author used K1 notation for the evaporite-bearing unit of the lower Keuper, and K4 and K5 notations for the two evaporite units of the upper Keuper, as used also in the Betic basin by Pérez-López (1996, 1998). To simplify terminology these notations are also used here for the equivalent units in the Catalan basin (Fig. 2): 'K1 units' refers to the Jarafuel Formation and the Miravet Formation, 'K4 units' to the Quesa Formation and Molar Formation, and 'K5 units' to the Ayora Formation and Gallicant Formation.

Several paleohighs controlled sedimentation in eastern Iberia during the Triassic (Castillo Herrador, 1974) (Fig. 1B). The most important were the NW-SE-oriented Ateca-Castelló high separating the Valencian sector of the Iberian basin in the south from the Maestrat sector in the north, and the NE-SW-oriented Lleida high that separated the Ebro basin to the west from the Catalan basin to the east.

A general view of the geographical distribution, composition, and sedimentology of the Triassic evaporites of eastern Iberia can be found in Ortí et al. (2017). The Ca-sulfate rocks of all these units consist of gypsum in outcrop, but anhydrite is predominant at depth. Several of these units include large masses of salt (halite) in the subsurface, which have promoted intense diapirism in several areas (Basque-Cantabrian and eastern Betic regions) during the Mesozoic's extensional pulses and subsequent Alpine orogeny (Klimowitz et al., 1999; Martínez del Olmo et al., 2015).

3. Palynologic dating of evaporite units

Precise dating of the Triassic evaporites in eastern Iberia is difficult to establish due to a lack of diagnostic macrofossils. Dating has been, therefore, mainly based on palynological associations found in the claystone and marls of evaporite units. A brief summary of the available results arranged by basins is provided below.

In the Betic basin, the majority of palynological determinations for the Keuper units in the External Zone (Prebetic and Subbetic zones) indicates Carnian-Norian ages (Pérez-López et al., 1991). The Zamoranos Formation was dated Rhaetian (Pérez-López et al., 2021b).

In the Valencian sector of the Iberian basin, the Röt unit was assigned to the Anisian, and the middle Muschelkalk unit to the middle-late Anisian (mainly Illyrian) in Ortí et al. (2020). Accordingly, the Röt unit probably has early Anisian age (Aegean). Also in this sector, all the Keuper units were assigned to the Carnian by Solé de Porta and Ortí (1982) and De Torres (1990). The Anhydrite Zone was dated Rhaetian in the Carcelén-1 borehole by Castillo Herrador (1974) and in the Domeño section (Chelva outcrop) by Pérez-López et al. (1996). In other areas of the Iberian basin, however, the Keuper units have been variably dated. Carnian-Norian or Norian ages have been proposed in the western and southwestern parts of the basin (Pérez-López et al., 1991; Arche and López-Gómez, 2014) and also in its central part (Doubinger et al., 1990). However, the lowest unit (K1) could be of a latest Ladinian-early Carnian age according to Doubinger et al. (1990) and

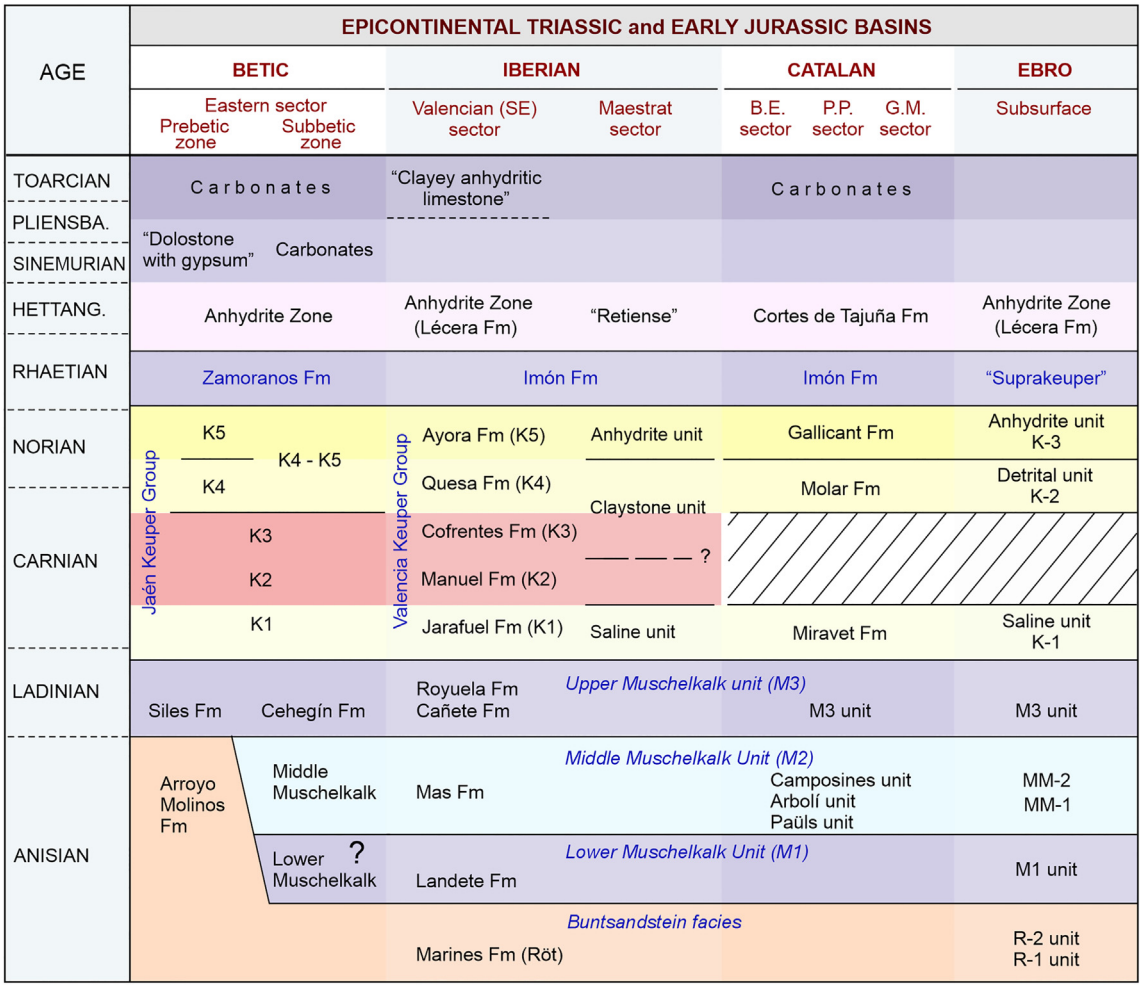

Fig. 2. Stratigrahic framework of the Epicontinental (Germanic) Middle-Upper Triassic in eastern Iberia, arranged by basins and basin sectors. The ages assigned to the stratigraphic units are approximate (Modified from Fig. 2 of Ortí et al., 2017). In order to distinguish the different evaporite units, a color has been added to all of them, which remains constant throughout the work.

Escudero-Mozo et al. (2015). The same Carnian-Norian or Norian ages have been proposed for the adjacent sectors of the Iberian basin such as the eastern Betic sector, the southeastern margin of the Stable Meseta (Besems, 1981a, 1981b) and the northeastern part of the Central System (Hernando, 1977) (Fig. 1A). For this reason, it is commonly assumed that in the Iberian basin and its adjacent sectors including the eastern Betic sector, the K1 unit is of latest Ladinian-early Carnian age, the siliciclastic K2 and K3 units of Carnian age, the K4 unit of late Carnian-early Norian age, and the K5 unit of Norian age (Fig. 2).

In the Catalan basin, the sediments equivalent to the Röt facies were dated early Anisian, the middle Muschelkalk unit was dated late Anisian, and the top beds of the upper Muschelkalk were dated 'probably Ladinian' in Calvet and Marzo (1994). Accordingly, the Anisian-Ladinian transition would correspond to the top of the middle Muschelkalk unit, and for this unit a late Anisian-early Ladinian age is assumed. The upper Muschelkalk unit has been dated as Ladinian-Cordevolian (base of the Carnian) by García-Ávila et al. (2020) and the lower Keuper unit (Miravet Formation) was assigned to the Carnian by Solé de Porta et al. (1987).

In the evaporitic Ballobar sub-basin of the Ebro basin (Fig. 1), the Röt facies was dated as Anisian (Ballobar-1 borehole) and the base of the Keuper unit as Ladinian (La Zaida borehole) by Jurado (1989, 1990). Also in this sub-basin, the base of the Anhydrite Zone was dated Rhaetian and the central-upper part as Hettangian by Castillo Herrador (1974). In the eastern part of the Pyrenean basin (External Serres and Nogueres sectors) some contradictory palynological data exist. Calvet et al. (1993) dated as Carnian the transition from the upper Muschelkalk unit to the Keuper facies, as Norian the basal unit of the Keuper and other units of the middle Keuper, and as Rhaetian the uppermost Keuper unit (K5). In the Nogueres sector, however, the Adons Formation (lower Keuper unit of Salvany and Bastida, 2004) was dated as upper Ladinian-Carnian by Fréchengues and Peybernès (1991) and Fréchengues et al. (1992).

In the Basque-Cantabrian basin, the lower Keuper unit (K1) was also dated Norian in Aguilar de Campoo, Reinosa, and Estella by Calvet et al. (1993), and the two upper Keuper units (K4, K5) were dated Rhaetian in the Poza de la Sal diapir (Ortí et al., 2017, their Table 3). Accordingly, and based mainly on Calvet et al. (1993), palynological dating in the Basque-Cantabrian basin, and possibly also in the western part of the Pyrenean basin, indicates that the Keuper units would be younger than in the other basins of eastern Iberia. In the Asturian basin, and also on the basis of palynological associations, the Rhaetian-Hettangian boundary has been located towards the base of the Anhydrite Zone, and the top of this unit is most probably of Pliensbachian age (Gómez et al., 2007).

As a result of these palynological data from the various Triassic basins in eastern Iberia, some diachronism possibly exists regarding the Keuper units. Thus, these units could be somewhat older towards the eastern (Mediterranean) sectors and younger towards the western and northwestern ones. However, it should be highlighted that the

samples documented isotopically in this study come from the easternmost basins and basin sectors in eastern Iberia, where diachronism should be less significant than for sampling in an east-to-west transect across eastern Iberia.

4. Materials and methods

The isotope data assemblage ($\delta^{34}S_{V\text{-}CDT}$, $\delta^{18}O_{V\text{-}SMOW}$) in the gypsum and anhydrite rocks here reported has a double provenance, 153 new sulfate isotope determinations and 223 previously published analyses. The stratigraphic intervals of the evaporite units documented isotopically in this paper are shown in Fig. 3. Arranged by stratigraphic units, the localities and outcrops of our sampling is indicated in Table 1. All data ($\delta^{34}S$, $\delta^{18}O$) assigned to specific evaporite units in this study (excluded 75 literature analyses of undifferentiated Keuper) are shown in isotope tables. Isotope mean values and standard deviations (Stdv) were calculated (from Excel© software) firstly for each outcrop or borehole, and these values used to calculate the mean values and Stdv for each basin sector. In turn, the latter values were used to calculate the mean values and Stdv for each basin. Finally, the basin values were used to calculate the mean values and Stdv for each evaporite unit.

All the reported samples come from outcrop, quarry walls, mine galleries, and lithologic cores either of deep oil boreholes (>1000 m) or shallower hydrogeologic boreholes (<1000 m). The gypsum samples always consist of 'secondary gypsum', i.e. gypsum derived from hydration near the surface of precursor anhydrite, which is ubiquitous at depth. The anhydrite samples are predominantly late diagenetic, i.e. derived from primary gypsum-to-diagenetic anhydrite conversion during deep burial, however, in some units they are early diagenetic sabkha products (without gypsum precursor; see below, Section 6.1).

The sulfur and oxygen isotope composition of the gypsum and anhydrite samples analyzed here (n = 153) were determined at the Scientific and Technological Centers (CCiTUB) of the Universitat de Barcelona. Samples were dissolved in distilled water, acidified to pH 3 by adding HCl (1:2), and then reprecipitated as barium sulfate by means of a solution of 5% $BaCl_2 \cdot 2H_2O$. The $\delta^{34}S\text{-}SO_4^{2-}$ was analyzed with a Carlo Erba EA coupled in continuous flow to a Finnigan

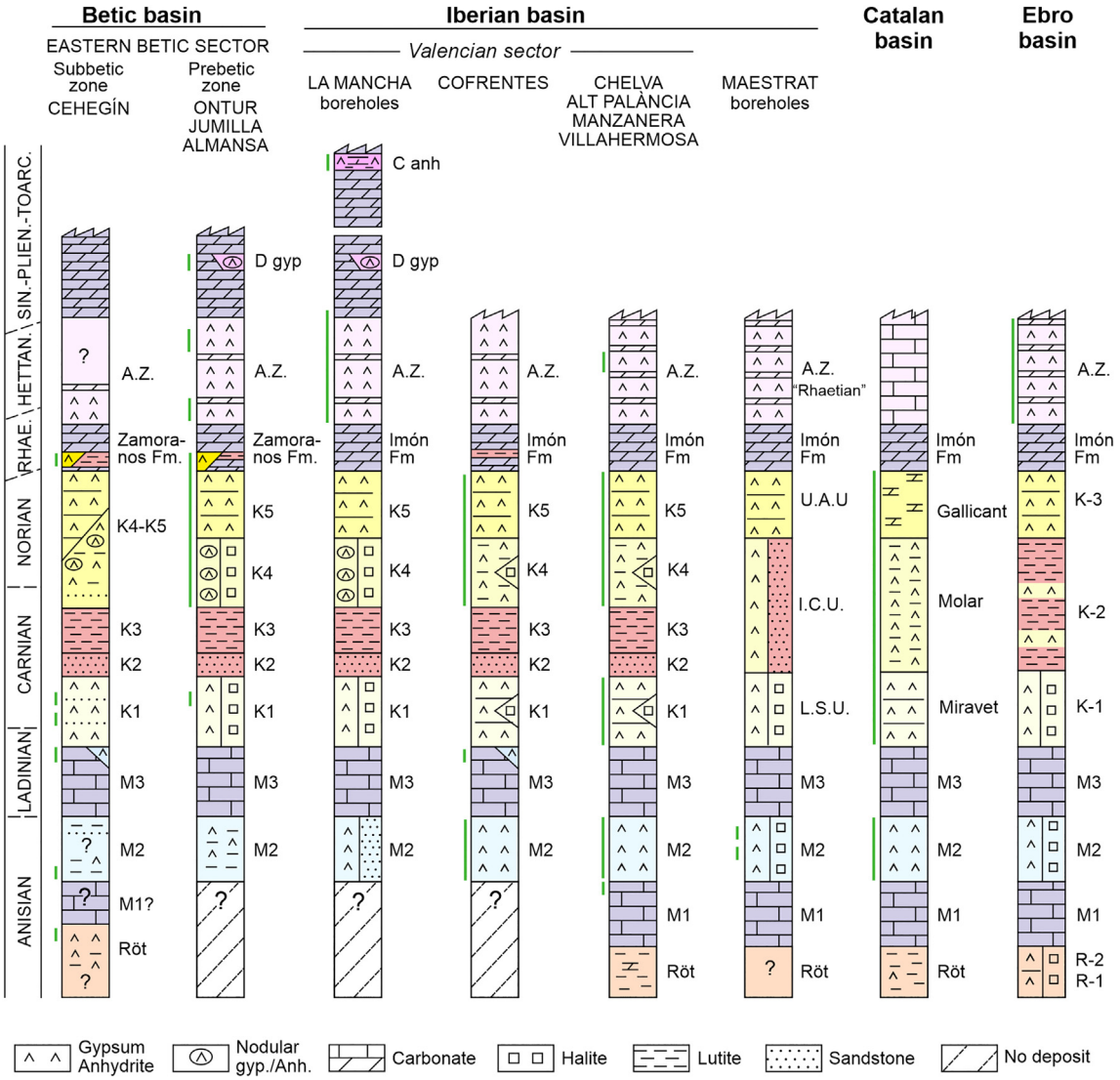

Fig. 3. General stratigraphic successions representative of the Middle Triassic to Early Jurassic in eastern Iberia. The ages assigned to the stratigraphic units are approximate. The stratigraphic intervals whose gypsum/anhydrite samples are documented isotopically are indicated by green vertical lines to the left of the sections. The stratigraphic units with evaporites, from older to younger, are: Röt; M1, lower Muschelkalk; M2, middle Muschelkalk; M3, upper Muschelkalk; K1, lower Keuper; K2 and K3, middle Keuper; K4 and K5, upper Keuper; Zamoranos Formation and lateral equivalent (Pérez-López et al., 2012, Imón Fm); A.Z., Anhydrite Zone; 'Dolostone with gypsum' (Dgyp); 'Clayey anhydritic limestone' (Canh). Nomenclature of the units: Betic and Iberian basins after Ortí et al. (2017) and Pérez-López (1996, 1998), Maestrat boreholes after Bartrina and Hernández (1990), Catalan basin after Salvany and Ortí (1987), Ebro boreholes (L.S.U., lower saline unit; I.C.U., intermediate clastic unit; U.A.U, upper anhydrite unit) after Jurado (1990).

Table 1
Localities of the new Ca-sulfate samples analyzed in this study.

Age	Units	Localities of the new samples (present study)
Early Jurassic	"Dolostone with gypsum" unit	- Ontur outcrop (eastern sector of the Betic basin).
	Anhydrite Zone	- Ontur outcrop (Albatana, eastern sector of the Betic basin). Chelva outcrop (Valencian sector of the Iberian basin). Alacón and Ezcaray boreholes (Aragonian sector of the Iberian basin).
Upper Triassic	Zamoranos Fm	- Calasparra outcrop (eastern sector of the Betic basin). Almansa castle (eastern sector of the Betic basin).
	Upper Keuper units (K4 and K5)	- Jumilla outcrop (eastern sector of the Betic basin). Pinoso diapir (eastern sector of the Betic basin). Ontur outcrop (Albatana, eastern sector of the Betic basin). Montealegre del Castillo outcrop (eastern sector of the Betic basin). Almansa outcrops (eastern sector of the Betic basin). Catalan basin (several stratigraphic sections in the three sectors).
	Lower Keuper units (K1)	- Jumilla outcrop (eastern sector of the Betic basin). Elche Reservoir outcrop (eastern sector of the Betic basin). Cofrentes, Chelva, Alt Palància and Manzanera outcrops (Valencian sector of the Iberian basin). Villel outcrop (Valencian sector of the Iberian basin). Catalan basin (several stratigraphic sections in the three sectors).
Middle Triassic	Upper Muschelkalk unit (M3, uppermost part)	- Cehegín outcrop (Argos Reservoir; eastern sector of the Betic basin). Cieza (Sierra del Oro outcrop, eastern sector of the Betic basin). - Calasparra outcrop (eastern sector of the Betic basin). - Cofrentes outcrop (Jarafuel section; Valencian sector of the Iberian basin).
	Middle Muschelkalk unit (M2)	- Cehegín outcrop (eastern sector of the Betic basin). - Chelva-Manzanera-Alt Palància outcrops (Valencian sector of the Iberian basin).
	Röt unit	- Cehegín outcrop (eastern sector of the Betic basin).

Delta XP Plus IRMS, whereas the $\delta^{18}O$-SO_4^{2-} was analyzed with a ThermoQuest high-temperature conversion analyzer (TC/EA) coupled in continuous flow to a Finnigan Matt Delta XP Plus IRMS. Results are reported in δ values relative to international standards (Vienna Canyon Diablo Troilite (VCDT) for $\delta^{34}S$ and Vienna Standard Mean Ocean Water (VSMOW) for $\delta^{18}O$. Analytical reproducibility by repeated analyses of both international and internal reference samples of known isotopic composition was determined to be about ±0.2‰ for $\delta^{34}S$, ±0.5‰ for $\delta^{18}O$ of SO_4^{2-}.

5. Isotope results

The $\delta^{34}S$ and $\delta^{18}O$ mean values and standard deviations for each unit arranged by basins and sectors are shown in Fig. 4. The $\delta^{34}S$-$\delta^{18}O$ diagrams for some evaporite units are shown in Fig. 5. For six of the units, the $\delta^{34}S$ and $\delta^{18}O$ profiles of mean values arranged by basins and sectors are shown in Fig. 6.

In the Röt unit (Table 2A), only two samples were available for analysis (Cehegín outcrop; eastern Betic sector; Fig. 1B). In these samples, $\delta^{34}S$ values were 17.5‰ and 17.9‰, and $\delta^{18}O$ values were 14.8‰ and 14.2‰ (Fig. 4).

For the middle Muschelkalk unit (Tables 2A, 2B, the mean values were 17.2 ± 0.5‰ for $\delta^{34}S$ (n = 107) and 13.5 ± 1.7‰ for $\delta^{18}O$ (n = 103). $\delta^{34}S$ isotope values varied from 15.6‰ to 18.8‰, while $\delta^{18}O$ values showed much wider variation from 7.6‰ to 22.0‰. The $\delta^{34}S$ mean values are slightly lower in the eastern Betic sector (17.1 ± 0.7‰) and the Valencian sector of the Iberian basin (16.6 ± 0.3‰) than in the Maestrat sector of this basin (17.4 ± 0.1) and the Catalan basin (17.8‰ ± 0.3). $\delta^{18}O$ mean values were higher in the Valencian sector of the Iberian basin (16.0 ± 1.0‰) than in the other basins and sectors studied (Fig. 4).

Towards the top of the upper Muschelkalk unit (n = 4; Table 3), gypsum beds intercalated within the carbonates/marls in several outcrops of the eastern Betic sector and the Valencian sector of the Iberian basin showed $\delta^{34}S$ mean value of 16.4 ± 0.2‰ and $\delta^{18}O$ mean value of 13.8 ± 0.3‰ (Fig. 4).

In the 'K1 units' (n = 51; Table 4), mean values of 15.1 ± 0.2‰ in $\delta^{34}S$ and 14.4 ± 1.4‰ in $\delta^{18}O$ were recorded. $\delta^{34}S$ mean values were relatively homogenous in the basins and sectors. $\delta^{18}O$ mean values recorded in the outcrops of the Valencian sector (Iberian basin) were 15.9 ± 0.8‰ (n = 29), higher than in other sectors and basins (Fig. 4).

In the 'K4 units' of the upper Keuper (n = 39; Table 5), mean values of 14.6 ± 0.3‰ for $\delta^{34}S$ and 14.2 ± 0.9‰ for $\delta^{18}O$ were recorded. In the outcrops of the Valencian sector of the Iberian basin, $\delta^{18}O$ mean values were higher (15.2 ± 1.3‰; n = 18) than in other sectors and basins, excluded the Priorat-Prades sector of the Catalan basin (Fig. 4, Table 5).

In the 'K5 units' of the upper Keuper (n = 46; Table 6), analyses yielded mean values of 14.9 ± 0.1‰ for $\delta^{34}S$ and 13.6 ± 0.7‰ for $\delta^{18}O$. With similar number of samples analyzed, this $\delta^{34}S$ mean value is slightly higher than that of the 'K4 units' (Fig. 4).

Literature isotope data for the group of undifferentiated Keuper facies were not assigned to any specific unit (Birnbaum and Coleman, 1979; Rouchy and Pierre, 1979; Utrilla et al., 1992; Gómez et al., 2004; Alonso-Azcárate et al., 2006; Gibert et al., 2007; Iribar and Ábalos, 2011; García Veigas et al., 2013; Ortí et al., 2014; Rossi et al., 2015; Ortí et al., 2020; Ortí et al., 2021; Ortí et al., 2021; Pérez-López et al., 2021a; Supplementary data, Tables 1S, 2S). For these gypsum/anhydrite samples (75 $\delta^{34}S$ analyses, 70 $\delta^{18}O$ analyses), individual values vary from 10.2 ‰ to 15.8‰ for $\delta^{34}S$ and from 10.4‰ to 17.9‰ for $\delta^{18}O$ (Supplementary Data, Tables 1S, 2S).

The gypsum layers intercalated towards the base of the Zamoranos Formation (n = 3; Table 7) in the outcrops of the eastern Betic sector showed mean values of 16.4 ± 0.1‰ for $\delta^{34}S$ and 13.3 ± 0.7‰ for $\delta^{18}O$. These $\delta^{34}S$ values are higher than those of the two upper Keuper units (Fig. 4).

For the Anhydrite Zone (Lécera Fm) (n = 35, Table 7), mean values were 14.2 ± 1.2‰ for $\delta^{34}S$ and 13.8 ± 3.8‰ for $\delta^{18}O$. The assemblage of individual $\delta^{34}S$ values for this unit, ranging from 11.5‰ to 16.3‰, is the lowest but also the most variable in the evaporite units of the present study. At the top of this unit, however, a $\delta^{34}S$ value of 16.3‰ was recorded at the Carcelén-1 borehole. Isotopic profiles of individual samples for some boreholes are shown in Fig. 7.

In the Early Jurassic carbonates overlying the Anhydrite Zone (Table 7), two main sulfate horizons are present. A lower one is

LITHOSTRATIGRAPHIC UNITS	MEAN VALUE → $\delta^{34}S$ → $\delta^{18}O$ (‰)	▲ BETIC BASIN Eastern Betic Sector: Prebetic zone	▲ BETIC BASIN Eastern Betic Sector: Subbetic zone	● IBERIAN BASIN: Castilian-Valencian Branch, Valencian sector	● IBERIAN BASIN: Castilian-Valencian Branch, Maestrat sector	● IBERIAN BASIN: Aragonian Branch	■ CATALAN BASIN: Baix Ebre sector	■ CATALAN BASIN: Priorat-Prades sector	■ CATALAN BASIN: Gaià Montseny sector	♦ EBRO BASIN: Boreholes
CLAYEY ANHYD. LIMESTONE	19.1 ±0.2 11.7 ±0.9 (2)			19.1 ±0.2 11.7 ±0.8 (2)						
DOLOSTONE WITH GYPSUM	16.4 ±0.1 14.6 ±0.2 (2)	16.4 ±0.1 14.6 ±0.2 (2)								
ANHYDRITE ZONE (AZ)	14.2 ±1.2 13.8 ±3.8 (35)	15.3 ±0.1 19.5 ±0.1 (2)		14.5 ±0.6 11.5 ±2.0 (11)		14.5 ±0.0 11.7 ±0.4 (16)				12.4 ±0.9 12.6 ±0.8 (6)
ZAMORANOS FORMATION	16.4 ±0.1 13.3 ±0.7 (3)	16.3 12.8 (2) 16.4 ±0.1 13.3 ±0.7 (3)	16.4 13.8 (1)							
UPPER KEUPER (K5)	14.9 ±0.1 13.6 ±0.7 (46)	14.5 ±0.4 12.5 ±1.7 (12)		14.6 ±0.6 13.6 ±2.9 (28)				15.6 ±0.3 14.7 ±1.2 (6)		
UPPER KEUPER (K4)	14.6 ±0.3 14.2 ±0.9 (39)	14.3 ±0.2 13.6 ±0.6 (5)		14.5 ±0.3 15.2 ±1.3 (18)			14.9 13.1 (4)	14.8 15.4 (5) 14.9 ±0.0 13.9 ±1.3 (16)	14.9 13.3 (7)	
LOWER KEUPER (K1)	15.1 ±0.2 14.4 ±1.4 (51)	14.4 15.2 (1) 14.9 ±0.7 14.3 ±0.9 (5)	15.15 13.9 (4)	15.1 ±0.3 15.9 ±0.8 (29)			15.4 13.8 (6)	15.4 ±0.0 13.0 ±1.2 (17)	15.3 12.1 (11)	
UPPER MUSCHELK. (M3)	16.4 ±0.2 13.8 ±0.3 (14)		16.3 ±0.1 13.6 ±0.6 (6)	16.5 ±0.6 14.0 ±1.1 (8)						
MIDDLE MUSCHELK. (M2)	17.2 ±0.5 (107) 13.5 ±1.7 (103)	16.6 11.5 (1) 17.1 ±0.7 12.6 ±1.5 (2)	17.6 13.6 (1)	16.6 ±0.3 16.0 ±1.0 (60)	17.4 ±0.1 12.7 ±0.4 (4)		17.6 12.8 (12)	18.1 13.3 (12) 17.8 ±0.3 (42) 12.7±0.7 (38)	17.7 11.9 (14)	
BUNTSAND. (Röt)	17.7 ±0.3 14.5 ±0.4 (2)	17.7 ±0.3 14.5 ±0.4 (2)								

Fig. 4. $\delta^{34}S$ and $\delta^{18}O$ (‰) mean values and standard deviations of the Middle Triassic-Early Jurassic evaporite units in eastern Iberia arranged by basins and basin sectors. Mean values: $\delta^{34}S$ in upper position, $\delta^{18}O$ in lower position. In brackets: number of samples.

interbedded within the Sinemurian-Pliensbachian succession in the eastern Betic sector (Prebetic zone; Ontur outcrop, Pérez-López et al., 1996, their Fig. 7). In this horizon, two gypsum samples yielded values of 16.3‰ and 16.4‰ for $\delta^{34}S$, and 14.4‰ and 14.7‰ for $\delta^{18}O$. The other horizon is interbedded within the top claystones and carbonates of the 'Middle Liassic' succession of the Carcelén-1 borehole (Castillo Herrador, 1974) which is located in the La Mancha area (west of the Valencian sector, Iberian basin) (Fig. 1A). Two anhydrite samples in this horizon yielded values of 18.9‰ and 19.2‰ for $\delta^{34}S$ and 11.1‰ and 12.3‰ for $\delta^{18}O$ (Utrilla et al., 1992). This clayey-carbonatic-sulfate horizon rests directly under the Dogger carbonates, and most probably has Toarcian age (Fig. 7).

Considering by basins the results here documented, the isotopic data are as follows. For the eastern sector of the Betic basin, the $\delta^{34}S$ and $\delta^{18}O$ profiles of mean values by units are shown in Fig. 8A, and profiles of individual sample values in some stratigraphic sections are shown in Fig. 8B. For the Valencian sector of the Iberian basin, profiles of $\delta^{34}S$ mean values in some outcrops show similar trends (Fig. 9A). In contrast, profiles of $\delta^{18}O$ mean values in three units (Fig. 9B) show very irregular trends. For the Catalan basin, profiles of mean values by units show decreasing and increasing trends for $\delta^{34}S$ and $\delta^{18}O$, respectively (Fig. 10A). Profiles of individual sample values in some stratigraphic sections are shown in Fig. 10B.

6. Isotope interpretation and possible relationships with global events

There is general agreement regarding the marine origin of most evaporites precipitated during the Middle-Late Triassic in several geological domains (Holser, 1977; Claypool et al., 1980; Holser et al., 1988; Strauss, 1997). Hence, sulfur and oxygen isotope values ($\delta^{34}S$, $\delta^{18}O$) of these sulfates represent those of the dissolved sulfate in the coeval marine brines. In eastern Iberia, this interpretation seems valid for the $\delta^{34}S$ values because of the similitude with those of the literature and their homogeneity. Some units display small $\delta^{34}S$ regional differences, in general between 1‰ and maximum 3‰, which could be assigned to local conditions of precipitation or small diachronism. For the $\delta^{18}O$ values, although they are more variable in each evaporite unit, they can be considered also primary signatures because of the similar variations reported in the literature for these values. Few samples, however, yielded anomalous $\delta^{18}O$ values and could be considered outliners or 'secondary' signatures.

6.1. The diagenetic cycle of the Ca-sulfate evaporites

The diagenetic cycle of Ca-sulfates in the evaporite deposits involves (1) the precipitation of gypsum from a concentrated solution ('primary gypsum'), (2) its dehydration into anhydrite during moderate to deep

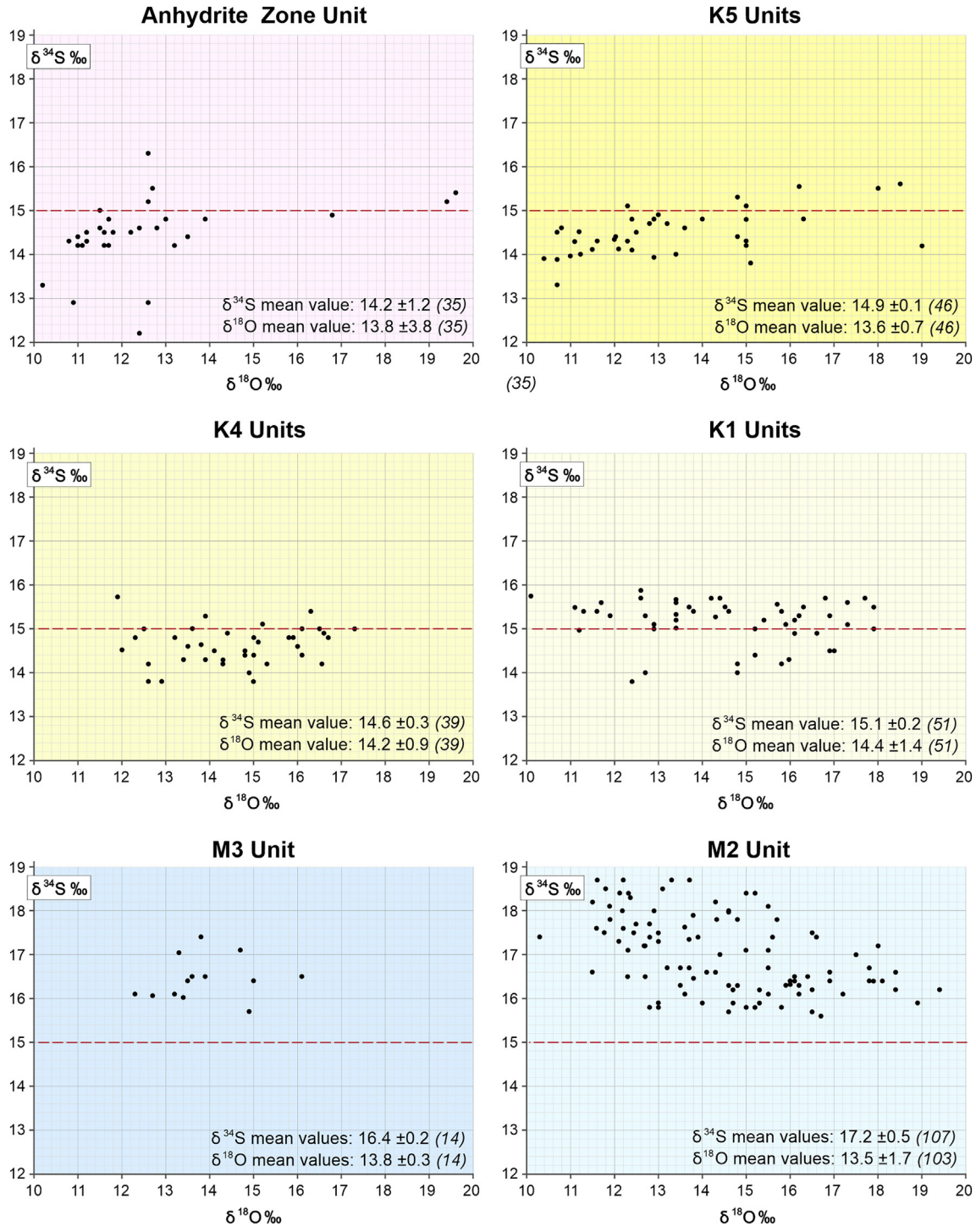

Fig. 5. $\delta^{34}S$ and $\delta^{18}O$ diagrams for some Middle Triassic-Early Jurassic evaporite units in eastern Iberia (see Fig. 4). All their reported samples are projected. The $\delta^{34}S$ 15.0 ‰ horizontal line is used as visual reference.

burial ('diagenetic anhydrite'), and (3) the rehydration of this anhydrite into gypsum near the surface during uplift ('secondary gypsum') (Murray, 1964; Mossop and Shearman, 1973). This cycle has entirely affected the Ca-sulfates of all Triassic evaporite successions in eastern Iberia (Ortí, 1974; Utrilla et al., 1992; Pérez-López et al., 1996; Playà et al., 2000; Salvany and Bastida, 2004; Ortí et al., 2014; among others). Probably the cycle has also entirely affected all the Triassic Ca-sulfates in the areas of Central-Western Europe (Dronkert, 1987; Dronkert et al., 1990; Boschetti et al., 2011). In the case, however, of primary or very early diagenetic (sabkha) anhydrite, the cycle reduces to the final anhydrite-to-secondary gypsum conversion.

Very few studies, however, have assessed the possible modifications in isotope compositions ($\delta^{34}S$, $\delta^{18}O$) of Ca-sulfate minerals throughout the cycle. Without mentioning the existence of this cycle, papers dealing with Triassic sulfate evaporites often assume that the isotope values in the analyzed samples represent $\delta^{34}S$ and $\delta^{18}O$ values of the original mineral. Effectively, according to Holser and Kaplan (1966) no significant differences have been detected in Ca-sulfate crystallizations that

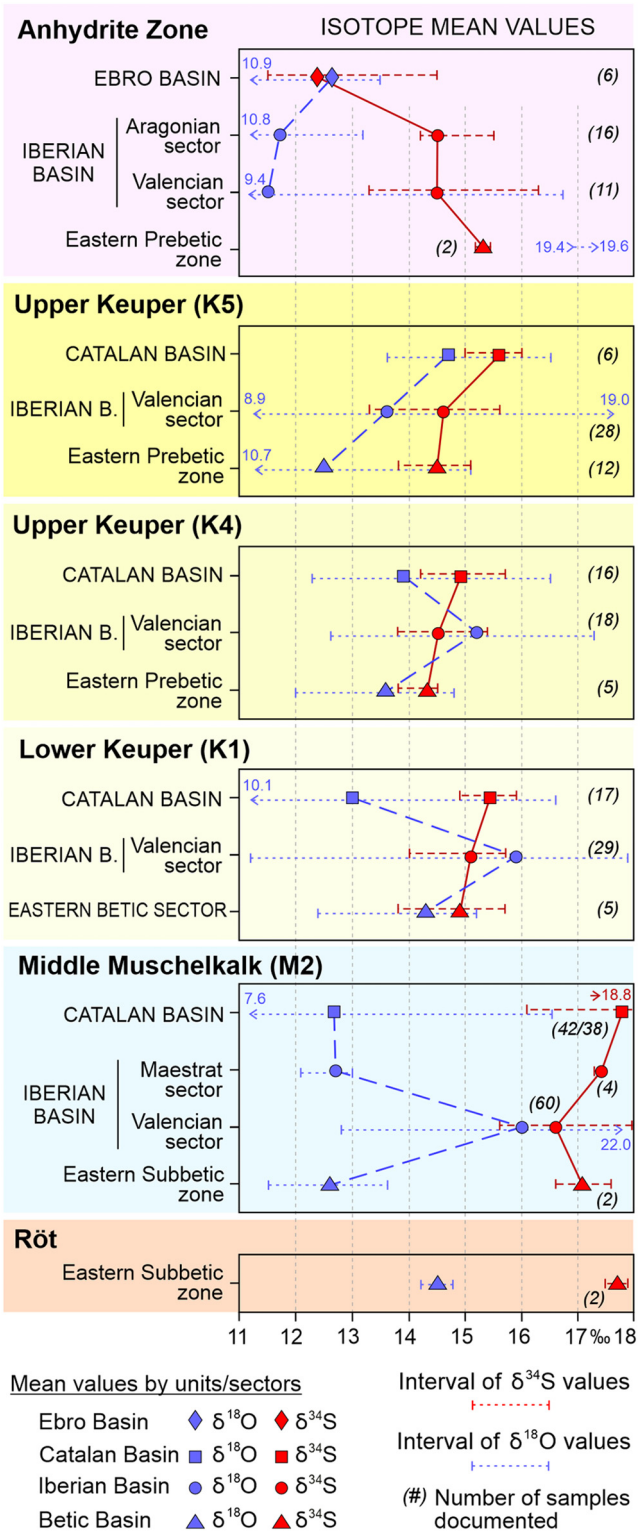

Fig. 6. Isotope trends of mean values ($\delta^{34}S$, $\delta^{18}O$) by evaporite units arranged by basins and basin sectors. Note the relative uniformity of the $\delta^{34}S$ trends and the variability of the $\delta^{18}O$ ones.

depend on mineralogy. Further, weathering of evaporites also occurs without isotope fractionation (Claypool et al., 1980). According to these observations, scarce changes in the isotopic signatures of the primary gypsum would be expected throughout the Ca-sulfate cycle.

Gypsum precipitation from a saturated solution occurs with enrichment of about 1.65‰ for $\delta^{34}S$ (Thode and Monster, 1965) and 3.5‰ for $\delta^{18}O$ (Lloyd, 1968) (see discussions in Raab and Spiro, 1991; Strauss, 1997, among others). However, possible enrichment for the primary precipitation of anhydrite has not yet been firmly established, mainly because of the difficulty in experimentally precipitating primary anhydrite (Hardie, 1967). With regard to the transformation of primary gypsum into diagenetic anhydrite, little -if any- modification in the $\delta^{34}S$ signature was detected by Worden et al. (1997) in their isotope study of the Kuff Formation in Abu Dhabi, a Late Permian-Early Jurassic carbonate unit bearing abundant anhydrite. This thick formation, estimated to have been deposited within ~5 Ma, has undergone up to 5000 m in burial, and remains devoid of significant subsequent uplift. In the thickness interval of ~700 m investigated by Worden et al. (1997), the $\delta^{34}S$ composition of the anhydrite rocks progressed from +10‰ in the Permian part of the succession to +20‰ in the Early Triassic part. The same increases were recorded in the $\delta^{34}S$ values of associated elemental sulfur and H_2S formed in this unit by the reaction of anhydrite with hydrocarbons via thermochemical sulfate reaction. According to Worden et al. (1997), these parallel evolution paths confirm that the original isotope signature for sulfur in the precursor gypsum has been preserved in rocks and fluids without significant changes.

For anhydrite rocks in other geological contexts, Spötl and Pak (1996) also observed that little, if any, $\delta^{34}S$ modification was detected in the anhydrite fragments of a severely deformed unit, the (Alpine) Haselgebirge 'tectonic mélange' of the Northern Calcareous Alps (Austria). According to Spötl and Pak (1996), the anhydrite rocks of this brecciated unit have preserved strong marine isotope signals despite having been affected by a number of physico-chemical processes in burial diagenesis and Alpine deformation. These observations indicate a resistance to the sulfur isotope composition changes of anhydrite formations under mechanical stress and/or fluid circulation.

As for the final transformation of burial anhydrite into secondary gypsum, we are unaware of studies specifically addressing the possible fractionation of sulfur and oxygen isotopes. However, no significant isotope differences for $\delta^{34}S$ have been reported in several articles dealing with evaporites of different age in eastern Iberia in which anhydrite and secondary gypsum coexist in borehole samples, outcrops and quarry walls (Playà et al., 2000; Carrillo et al., 2014; Ortí et al., 2014).

In absence of more specific research on possible isotope fractionation throughout the diagenetic cycle of the Ca-sulfates, it can be assumed that no substantial modifications in the original isotopic signatures -of primary gypsum or primary/very early diagenetic anhydrite- might be expected.

6.2. Significance of the Triassic isotope values

The $\delta^{34}S$ values recorded in this study for eastern Iberia are rather consistent across units, basins, basin sectors, and outcrops for the majority of evaporite units. Similarly, standard deviations are small, in general <0.5‰ and the scatter of individual values in the different outcrops and basin sectors is narrow. These values are interpreted as primary isotope signatures. Profiles of the $\delta^{34}S$ mean values produced over time in the evaporite units of the different basins are shown in Fig. 11.

The $\delta^{18}O$ values recorded in eastern Iberia are more variable than those of $\delta^{34}S$ (Fig. 11). These values, however, seem relatively consistent with the $\delta^{18}O$ values recorded for the same time interval in other basins in Central-Southern Europe (see below, Section 7) considered primary (unaltered) marine signals. However, the high standard deviations, often >1.0‰, and the wide scatter, of up to 5‰ or more, of individual values in some sectors and outcrops (Figs. 9B and 10B) suggest that some modifications of the original signals could have occurred locally.

Table 2A
Isotopic data ($\delta^{34}S$, $\delta^{18}O$) of the Röt unit and the middle Muschelkalk evaporite units of the Catalan basin documented in this study.

Unit basin/*sector*/outcrop	n	Lab. sample No.	Field sample name	Lithology	Occurrence	$\delta^{34}S$ (‰)	$\delta^{18}O$ (‰)	Mean $\delta^{34}S$ (‰)	Mean $\delta^{18}O$ (‰)	Stdv $\delta^{34}S$ (‰)	Stdv $\delta^{18}O$ (‰)	Ref.
- Röt unit								**17,7**	**14,5**	**0,3**	**0,4**	
Maximun value:						17,9	14,8					
Mininum value:						17,5	14,2					
Eastern Betic sector	***2***							***17,7***	***14,5***	***0,3***	***0,4***	
Cehegín (Subbetic)	2	387	19F-13	G	os	17,9	14,2					1
		388	19F-14	G	os	17,5	14,8					1
- Middle Muschelkalk	**107/ 103**							**17.2**	**13.5**	**0.5**	**1.7**	
Maximum value								18.8	22.0			
Minimum value								15.6	7.6			
Catalan basin	**41/37**							**17.8**	**12.7**	**0.3**	**0.7**	
A. Baix Ebre sector	***12***							***17.6***	***12.8***	***0.7***	***0.9***	
Paüls			MPA-4	G	qs	17.4	10.3	*18.1*	*12.2*	*0.4*	*1.5*	4
			MPA-3	G	qs	18.4	15.0					4
			MPA-1	G	qs	18.2	11.5					4
			Paüls-1	G	qs	18.0	12.2					4
			Paüls-2	G	qs	18.4	12.1					4
			Paüls-3	G	qs	18.4	12.3					4
Venta de Camposines			MVC-6	G	os	16.7	13.5	*17.1*	*13.5*	*0.6*	*1.2*	4
			MVC-8	G	os	16.5	12.7					4
			MVC-9	G	os	16.6	14.3					4
			VC-1	G	os	17.5	12.4					4
			VC-2	G	os	17.1	12.3					4
			MVC-2	G	os	18.1	15.5					4
B. Priorat-Prades sector	***16***							***18.1***	***13.3***	***0.3***	***0.6***	
Masriudoms			MMR-1	G	os	18.7	11.6	*18.1*	*14.1*	*0.8*	*3.5*	4
			MMR-2	G	os	17.5	16.5					4
Pratdip			MPT-2	G	o	18.5	13.1	*18.5*	*13.1*	-	-	4
Pradell			MPR-2	G	qs	18.2	14.3	*18.5*	*13.8*	*0.4*	*0.7*	4
			MPR-3	G	qs	18.7	13.3					4
Coll de Falset			MCF-2	G	os	18.0	12.9	*17.9*	*12.4*	*0.1*	*0.7*	4
			MCF-1	G	os	17.8	11.9					4
Arbolí			MAR.3	G	os	17.5	13.0	*18.1*	*13.3*	*0.6*	*1.7*	4
			MAR.10	G	os	18.4	15.2					4
			MAR.1	G	os	18.5	11.8					4
Rojalons			MRO-2	G	os	18.7	13.7	*18.0*	*13.2*	*1.1*	*0.7*	4
			MRO-3	G	os	17.2	12.7					4
Rojalons			RJ(2)	A	os	16.1	-	*17.6*	-	*1.1*	-	7
			RJ(3)	A	os	17.9	-					7
			RJ(4)	A	os	17.8	-					7
			RJ(5)	A	os	18.8	-					7
C. Gaià-Montseny sector	***13***							***17.7***	***11.9***	***0.3***	***1.6***	
Querol			MQE-5	G	os	16.5	12.3	*17.7*	*13.0*	*1.1*	*1.4*	4
			MQE-13	G	os	18.0	14.6					4
			MQE-8	G	q	18.7	12.2					4
Corbera			MFP-5	G	os	17.7	12.5	*17.7*	*12.5*	-	-	4
Vallirana			MVA-3	G	m	18.3	12.4	*18.2*	*12.1*	*0.1*	*0.3*	4
			MVA-5	G	m	18.1	11.9					4
La Puda			MLP-7	G	m	18.4	9.8	*17.8*	*8.7*	*0.9*	*1.5*	4
			MLP-4	G	o	17.1	7.6					4
Figaró			MFG-2	G	os	17.6	11.6	*17.7*	*12.9*	*0.2*	*1.4*	4
			MFG-4	G	os	17.5	11.8					4
			F-1	G	os	17.8	14.3					4
			F-2	G	os	17.9	13.8					4
Aiguafreda			MMC-1	G	os	17.2	12.7	*17.4*	*12.5*	*0.3*	*0.4*	4

Lithlogy: G, gypsum; A, Anhydrite. **Occurrence of the sample:** o, outcrop; os, stratigraphic section; q, quarry; qs, quarry section; db; deep borehole. **Stdv:** standard deviation. **Ref.:** 1, This study; 4, Ortí et al., 2018; 7, Morad et al., 1995.

6.3. Middle Triassic evaporites

An average $\delta^{34}S$ value of ~11.5‰ is commonly assumed for the late stage (Lopingian) of the Permian (Insalaco et al., 2006; Longinelli and Flora, 2007). At the Permian-Triassic boundary, values from ~11‰ to ~16‰ have been obtained by Worden et al. (1997) and Horacek et al. (2010), and significantly higher values ranging from ~16‰ to ~32‰ have been recorded for the early stage (Induan) of the Early Triassic by Worden et al. (1997) and Insalaco et al. (2006). This important $\delta^{34}S$ positive excursion has been linked to the major mass extinction at the Permian-Triassic boundary caused by global warming and drastic oceanic anoxia (Berner, 2005; Sun et al., 2012; Scotese et al., 2021). Subsequently to this positive shift, a sharp decrease (~17‰) has been obtained by Cortecci et al. (1981) at the Olenekian-Anisian (Early-Middle Triassic) transition. During the Anisian, $\delta^{34}S$ values between ~18‰ and ~25‰ have been reported by several authors (Cortecci et al., 1981; Spölt, 1988; Pearson et al., 1991; Bernasconi et al., 2017).

Table 2B
Isotopic data ($\delta^{34}S$, $\delta^{18}O$) of the middle Muschelkalk evaporite units of the Iberian and Betic basins documented in this study (continuation of Table 2A).

Unit basin/*sector*/outcrop	n	Lab. sample no.	Field sample name	Lithology	Occurrence	$\delta^{34}S$ (‰)	$\delta^{18}O$ (‰)	Mean $\delta^{34}S$ (‰)	Mean $\delta^{18}O$ (‰)	Stdv $\delta^{34}S$ (‰)	Stdv $\delta^{18}O$ (‰)	Ref.
Iberian basin	**64**							**17.0**	**14.3**	**0.6**	**2.3**	
A. Valencian sector	***60***							***16.6***	***16.0***	***0.3***	***1.0***	
Cofrentes	3	307	FE-12	G	o	16.4	16.0	*16.6*	*16.3*	*0.7*	*0.3*	1
		505	Ay4.0	G	o	17.4	16.6					1
		507	Ay4.7	G	o	16.1	16.2					1
Chelva	9	154	Ys.Ch-4	G	o	16.1	15.5	*16.3*	*14.9*	*0.5*	*1.1*	5
		315	Ys.Ch-21	G	os	15.9	14.0					1
		316	Ys.Ch-22	G	os	15.9	13.0					1
		319	Ys.Ch-25	G	os	16.3	14.8					1
		321	Ys.Ch-27	G	os	17.4	15.6					1
		322	Ys.Ch-28	G	os	16.7	13.7					1
		323	Ys.Ch-29	G	os	15.8	15.8					1
		414	Ys.Ch-37	G	os	16.2	15.3					1
		487	Ch-49	G	o	16.3	16.2					1
Alt Pallància	24	117	YsAt-18	G	o	15.6	16.7	*16.4*	*15.5*	*0.6*	*1.4*	5
		182	YsAt-27	G	o	16.4	18.1					5
		116	YsAt-14	G	o	17.4	15.6					5
		119	YsAt-16	G	o	16.3	14.6					5
		126	Bj-2	G	o	15.8	12.8					5
		324bis	YsAt-28	G	o	17.1	15.5					5
		102	To-1	G	o	16.6	14.1					5
		125	To-2	G	o	15.8	15.0					5
		115	YsAt-13	G	o	16.7	13.2					5
		104	M.MN-1	G	o	16.5	16.1					5
		133	M.MN-2	G	o	16.3	15.9					5
		127	MN-1	G	o	16.1	13.6					5
		174	YsAt-23	G	o	17.8	15.7					5
		175	YsAt-24	G	o	17.2	18.0					5
		171	YsAt-5	G	q	16.4	16.1					5
		137	YsAt-6	G	o	16.7	15.5					5
		138	YsAt-7	G	os	15.7	16.5					5
		373	Alt.4	G	os	16.3	16.0					1
		378	Alt.9	G	o	16.5	13.8					1
		479	Alt-24	G	o	15.9	14.7					1
		480	Alt-25	G	o	15.9	15.3					1
		481	Alt-26	G	o	15.7	14.6					1
		493	Alt-27	G	o	16.1	17.2					1
		494	Alt-28	G	o	16.4	17.6					1
Fanzara	2	164	Ys.At-20	G	o	16.6	16.9	*16.4*	*17.7*	*0.3*	*1.1*	5
		165	YsAt-	G	o	16.2	18.4					5
Villahermosa	4	148	Ys.Vl-4	G	o	16.7	17.8	*17.1*	*15.2*	*0.8*	*1.8*	5
		170	Ys.Vll-5	G	o	16.2	14.7					5
		383	Vll.7	G	o	18.0	14.6					1
		384	Vll.8	G	o	17.4	13.7					1
Manzanera	18	128	YsMz-13	G	o	17.1	15.0	*16.6*	*16.2*	*0.6*	*2.5*	1
		183	Ys.Mz-31	G	o	15.8	22.0					1
		143	YsMz-1	G	o	16.6	18.4					1
		132	YsMz-2	G	o	17.0	14.4					6
		107	YsMz-3	G	o	16.2	16.5					6
		184	Ys.Mz-33	G	o	17.0	17.5					1
		158	YsMz-1	G	o	16.4	17.9					1
		159	YsMz-11	G	o	17.4	13.9					1
		124	YsMz-12	G	o	16.3	13.5					1
		123	YsMz-5	G	o	15.8	15.2					1
		110	YsMz-9	G	o	15.8	13.0					6
		146	YsMz-21	G	o	16.5	16.4					6
		160	YsMz-22	G	o	16.4	17.8					6
		172	YsMz-25	G	o	16.2	19.4					1
		173	YsMz-27	G	o	15.9	18.9					1
		325	YsMz-34	G	o	17.1	15.0					1
		310	YsSCM-8	G	q	17.8	14.8					1
		312	YsSCM-10	G	q	17.7	12.8					1
B. Maestrat sector	***4***							***17.4***	***12.7***	***0.1***	***0.4***	
Bobalar borehole	4		M2-c10	A	db	17.5	13.0	*17.4*	*12.7*	*0.1*	*0.4*	2
			M5-c10	A	db	17.4	12.8					2
			M13-c11	A	db	17.3	13.0					2
			M14-c11	A	db	17.3	12.1					2
Betic Basin												
Eastern Betic Sector	**2**							***17.1***	***12.6***	***0.7***	***1.5***	
Jaraco borehole (Pre.)	1		1184.8 m	A	db	16.6	11.5	*16.6*	*11.5*	-	-	2
Cehegín (Sub.)	1	386	19-6	G	os	17.6	13.6	*17.6*	*13.6*	-	-	2

Lithlogy: G, gypsum; A, Anhydrite. **Occurrence of the sample:** o, outcrop; os, stratigraphic section; q, quarry; qs, quarry section; db; deep borehole. **Stdv:** standard deviation. **Ref.:** 1, This study; 2, Utrilla et al., 1992; 5, Ortí et al., 2020; 6, Pérez-López et al., 2021a. Betic zones: Pre., Prebetic zone; Sub., Subbetic zone.

Table 3
Isotopic data ($\delta^{34}S$, $\delta^{18}O$) of the upper Muschelkalk evaporite unit of eastern Iberia documented in this study.

Unit basin/*sector*/outcrop	n	Lab. sample no.	Field sample name	Lithology	Occurrence	$\delta^{34}S$ (‰)	$\delta^{18}O$ (‰)	Mean $\delta^{34}S$ (‰)	Mean $\delta^{18}O$ (‰)	Stdv $\delta^{34}S$ (‰)	Stdv $\delta^{18}O$ (‰)	Ref.
- Upper Muschelkalk	**14**							**16.4**	**13.8**	**0.2**	**0.3**	
Maximum value						17.4	16.1					
Minimum value						15.7	12.3					
Eastern Betic sector (Subbetic zone)	***6***							***16.3***	***13.6***	***0.1***	***0.6***	
Argos	2		12-22AG	G	o	16.4	13.5	*16.5*	*13.7*	*0.1*	*0.3*	3
		558	12-23A	G	os	16.5	13.9					1
Sierra del Oro	2	560	21F-Y30	G	os	16.5	13.6	*16.3*	*13.0*	*0.3*	*0.9*	1
		562	21F-Y32	G	os	16.1	12.3					1
Calasparra	2	566	21F-Y36	G	os	16.1	13.2	*16.3*	*14.1*	*0.2*	*1.3*	1
		567	21F-Y37	G	os	16.4	15					1
Valencian sector (Iberian Basin)	***8***							***16.5***	***14.0***	***0.6***	***1.1***	
Cofrentes	8	302	FE-1	G	o	16.5	16.1					1
		304	FE-1	G	o	17.1	14.7					1
		305	FE-6	G	o	15.7	14.9					1
		402	Ay4.2	G	os	17.0	13.3					1
		404	Ay4.4	G	os	16.1	12.7					1
		401	Ay4.1	G	os	17.4	13.8					1
		403	Ay4.3	G	os	16.5	13.3					1
		405	Ay4.5	G	os	16.0	13.4					1

Lithlogy: G, gypsum; A, Anhydrite. **Occurrence of the sample:** o, outcrop; os, stratigraphic section; q, quarry; qs, quarry section; db; deep borehole. **Stdv:** standard deviation. **Ref.:** 1, This study; 3, Ortí et al., 2014.

Somewhat different $\delta^{34}S$ values, however, were obtained by us for the Anisian samples. The two values (~18‰) reported for the Röt unit, probably of early Anisian (Agenian) age, agree with those obtained by Cortecci et al. (1981) for the Olenekian-Anisian boundary (~18‰). With regard to the middle Muschelkalk unit, of middle-late Anisian age -but most probably late Anisian (Illyrian substage)-, its values ranging from ~18‰ to ~16.5‰ are also lower than those in the literature.

Small differences in $\delta^{34}S$ means values were recorded in the different basins of eastern Iberia. The Catalan basin shows a very consistent set of $\delta^{34}S$ values, which seem to be the most complete for all the basins here documented (Ortí et al., 2018) (Fig. 10). These data indicate decreasing $\delta^{34}S$ mean values from the oldest subunit (Paüls Gypsum; 18.3‰) to the intermediate (Arbolí Gypsum; 17.7‰) and the youngest subunit (Camposines Gypsum; 16.6‰). In contrast, the $\delta^{18}O$ mean values show increasing trend from the basal to the upper subunit (12.3‰, 12.9 ‰ and 13.2‰, respectively). All these isotope compositions are considered primary signals. However, the $\delta^{34}S$ mean values of the Catalan basin differ slightly from those in the Betic basin and the Valencian sector of the Iberian basin (17.1±0.7‰ and 16.6±0.3‰, respectively) (Fig. 4). Accordingly, the Anisian evaporites of the latter basins could be somewhat younger than the oldest subunit (Paüls Gypsum) in the Catalan basin, where the ~18‰ value is largely represented (Table 2A).

6.4. Late Triassic evaporites

The lowest $\delta^{34}S$ mean value recorded by us for the upper Keuper sulfates was 14.6 ± 0.3‰ in the K4 units. This mean value corresponds to new evaporites precipitated immediately after the Carnian Pluvial Event (CPE). In eastern Iberia, this humid event is represented by the K2 and K3 units of the middle Keuper (Arche and López-Gómez, 2014). The event duration was of ~1.2 Ma and it took place towards the Carnian-Tuvalian transition (~234 Ma to ~232 Ma). The event, including at least four episodes of increased rainfall, is evidenced by repeated perturbations in the C cycle with negative $\delta^{13}C$ isotope excursions (Dal Corso et al., 2020). In turn, the CPE was linked to a major extinction crisis of marine and continental biota coincident with climate warming and possible oceanic anoxia. The ultimate control of the mass extinction was likely the eruption of the Wrangellia Large Igneous Province (LIP) in the Panthalassa ocean, which could have increased the greenhouse effect (Dal Corso et al., 2020). Although the possible influence of this event on the $\delta^{34}S$ values of the upper Keuper sulfates in eastern Iberia is not clear, a change from decreasing to increasing trend was observed in the sulfur isotope mean values ($\delta^{34}S$) from the lower (K4) to the upper (K5) units of the upper Keuper (Fig. 4). The lowest $\delta^{34}S$ mean value in the K4 units suggests evaporite precipitation from marine brines mixed with supplies of meteoric water. Some studies also assume a change from decreasing to increasing trend in the $\delta^{34}S$ values for the Norian evaporites in Central-Western Europe (Bernasconi et al., 2017).

The $\delta^{34}S$ values obtained here for the Zamoranos Formation (Rhaetian), of up to 16.4 ± 0.1‰, should be highlighted (Figs. 4, 8). Some authors have reported very sharp positive value excursions for $\delta^{34}S$ and $\delta^{13}C_{org}$ in marine sediments of Rhaetian age and have linked this perturbation of the sulfur and carbon cycles to the end-Triassic mass extinction. Williford et al. (2009) examined $\delta^{34}S_{VCDT}$ compositions in the reduced sulfate fraction (mainly pyrite) of Late Triassic-Early Jurassic marine sediments in British Columbia (Canada). These authors suggested that the $\delta^{34}S$ isotope shift was initiated by 'declining seawater sulfate concentration' due to evaporite deposition in nascent Atlantic rift zone. He et al. (2020) examined three open marine CAS-$S^{34}S$ profiles in stratigraphic successions from Tethyan and Panthalassan locations spanning the Norian to lower Hettangian. The three profiles showed similar trends, namely a large positive shift >10‰ (from ~16‰ up to ~31‰ in the Tethyan profile) and estimated duration of ~50 ka in the late Rhaetian. This $\delta^{34}S_{CAS}$ excursion was assigned to a major pyrite burial event driven by a large scale increase in oceanic anoxia during the late Rhaetian. The interpretation by He et al. (2020) involves a number of interdependent processes. Episodes of significant evaporite precipitation in a sulfate-rich ocean, either by rifting or other climatic/geodynamic cause, would result in the subsequent depletion of sulfate in the marine water. The coincidence with large episodes of volcanism leading to generalized warming (hothouse effect) would trigger (i) oceanic anoxia and associated biological crises, and (ii) intense pyrite burial deposition and associated heavier values of sulfur isotopes in the marine sulfate. He et al. (2020) calculated that the development of a low sulfate ocean (<1 millimolar) in the Late Triassic was driven by substantial evaporite deposition from marine water containing ~13 millimolar or even more sulfate during the Carnian. Coeval

Table 4
Isotopic data ($\delta^{34}S$, $\delta^{18}O$) of the evaporites in the lower Keuper units (K1) of eastern Iberia documented in this study.

Unit basin/*sector*/outcrop	n	Lab. sample no.	Field sample name	Lithology	Occurrence	$\delta^{34}S$ (‰)	$\delta^{18}O$ (‰)	Mean $\delta^{34}S$ (‰)	Mean $\delta^{18}O$ (‰)	Stdv $\delta^{34}S$ (‰)	Stdv $\delta^{18}O$ (‰)	Ref.
- Lower Keuper (K1)	**51**							**15.1**	**14.4**	**0.2**	**1.4**	
Maximum value:						15.9	17.9					
Minimum value:						13.8	10.1					
Betic Basin	**5**							**14.9**	**14.3**	**0.7**	**0.9**	
A. Eastern Prebetic sector	**1**							***14.4***	***15.2***	**-**	**-**	
Jumilla	1	538	21-45	G	os	14.4	15.2					1
B. Eastern Subbetic sector	**4**							***15.15***	***13.9***	***0.8***	***0.6***	
Calasparra	2		GSP-1	G	o	15.4	14.6	*14.6*	*13.5*	*1.1*	*1.6*	3
			GSP-2	G	o	13.8	12.4					3
Pantano de Elche	2	554	21-46	G	os	15.7	14.2	*15.7*	*14.3*	*0.0*	*0.1*	1
		557	21-49	G	os	15.7	14.4					1
Valencian sector (Iberian Basin)	***29***							***15.1***	***15.9***	***0.3***	***0.8***	
Cofrentes	2	301	FE-7	G	o	15.1	17.3	*15*	*16.7*	*0.1*	*0.8*	1
		306	FE-8	G	o	14.9	16.1					1
Chelva	10	149	Ys.Ch-1	G	o	15.2	15.4	*15.4*	*14.5*	*0.3*	*1.8*	5
		153	Ys.Ch-2	G	o	15.6	17.3					5
		152	Ys.Ch-7	G	os	15.5	13.7					5
		324	Ys.Ch-8	G	os	15.3	16.2					1
		328	Ys.Ch-12	G	os	15.6	13.4					1
		314	Ys.Ch-20	G	os	15.0	15.2					1
		318	Ys.Ch-24	G	os	15.7	12.6					1
		407	Ys.Ch-31	G	os	15.3	14.3					1
		412	Ys.Ch-35	G	o	15.0	11.2					1
		406	Ys.Ch-30	G	os	15.6	15.7					1
Alt Palància	7	101	Bj-1	G	o	14.3	16.0	*14.8*	*15.9*	*0.6*	*1.0*	5
		113	YsAt-10	G	o	15.5	16.3					5
		114	YsAt-11	G	o	14.0	14.8					5
		105	MN-2	G	o	15.5	14.5					1
		140	YsAt-3	G	o	14.5	17.0					5
		141	YsAt-4	G	o	14.5	16.9					5
		139	YsAt-8	G	os	15.2	16.1					5
Manzanera	8	156	YsMz-14	G	o	15.0	17.9	*14.9*	*16.2*	*0.7*	*1.8*	6
		142	YsMz-15	G	o	15.1	15.9					1
		168		G	o	15.5	17.9					1
		129	YsMz-16	G	os	14.0	12.7					6
		145	YsMz-7	G	o	15.7	17.7					6
		161	YsMz-23	G	o	14.2	15.8					1
		162	Ys.Mz-24	G	o	14.2	14.8					1
		163	YsMz-26	G	o	15.3	16.9					1
Villel	2	495	TER-1	G	os	15.4	15.2	*15.6*	*16.0*	*0.2*	*1.1*	
		497	TER-2	G	os	15.7	16.8					
Catalan Basin	**17**							**15.4**	**13.0**	**0.0**	**1.2**	
A. Baix Ebre sector	6		RA-12	G	o	14.9	16.6	***15.4***	***13.8***	***0.4***	***1.4***	4
		426	KMI-1	G	os	15.9	12.6					1
		428	KMI-3	G	os	15.7	13.4					1
		430	KMI-5	G	os	15.3	13.4					1
		427	KMI-2	G	os	15.7	13.6					1
		429	KMI-4	G	os	15.2	13.4					1
B. Gaià-Montseny sector	***11***		ES-5	G	os	15.1	12.9	***15.3***	***12.1***	***0.2***	***1.1***	4
			ES-7	G	os	15.4	13.8					4
			ES-14	A	os	15.3	12.7					4
		437	KCO-2	G	os	15.6	11.7					1
			CO-3	G	os	15.4	11.3					4
			CO-16	G	os	15.3	11.9					4
			MG-1	G	o	15.4	11.6					4
			MG-3	G	o	15.0	12.9					4
		453	KCO-1	G	os	15.8	10.1					1
		454	KCO-3	G	os	15.5	11.1					1
		455	KCO-4	G	os	15.0	13.4					1

Lithlogy: G, gypsum; A, Anhydrite. **Occurrence of the sample*:*** o, outcrop; os, stratigraphic section; q, quarry; qs, quarry section; db; deep borehole. **Stdv:** standard deviation**. Ref.:** 1, This study; 3, Ortí et al., 2014; 4, Ortí et al., 2018; 5, Ortí et al., 2020; 6, Pérez-López et al., 2021a.

volcanism triggering the interrelated processes would correspond to the first activity stages in the Central Atlantic Magmatic Province (CAMP). With regard to eastern Iberia, few localities with Rhaetian evaporites were found up until now by us. However, all they include volcano-genetic deposits which have been linked to the activity of the Central Atlantic Magmatic Province by Pérez-López et al. (2021b). The Rhaetian $\delta^{34}S_{VCDT}$ positive excursion provided in this study analyzing gypsum rocks could be related to others obtained analyzing non-evaporitic sediments (Williford et al., 2009; He et al., 2020).

6.5. Early Jurassic evaporites

Also the low $\delta^{34}S$ values of the Anhydrite Zone (Rhaetian-Hettangian-Sinemurian) and their variability should be highlighted.

Table 5
Isotopic data ($\delta^{34}S$, $\delta^{18}O$) of the evaporites in the lower unit of the upper Keuper (K4) of eastern Iberia documented in this study.

Unit basin/*sector*/outcrop	n	Lab. sample No.	Field sample name	Lithology	Occurrence	$\delta^{34}S$ (‰)	$\delta^{18}O$ (‰)	Mean $\delta^{34}S$ (‰)	Mean $\delta^{18}O$ (‰)	Stdv $\delta^{34}S$ (‰)	Stdv $\delta^{18}O$ (‰)	Ref.
- Upper Keuper (K4)	**39**							**14.6**	**14.2**	**0.3**	**0.9**	
Maximum value:						15.7	17.3					
Minimum value:						13.8	11.9					
Eastern Betic sector (Prebetic zone)	***5***							***14.3***	***13.6***	***0.2***	***0.6***	
Jumilla	2	389	1	G	qs	14.3	14.3	*14.4*	*13.2*	*0.2*	*1.6*	1
		390	2	G	qs	14.5	12.0					1
Montealegre	1	533	21-58	G	qs	13.8	13.0	*14.1*	*14.0*	*0.3*	*0.9*	1
Almansa (Buenavista)	1	515	21-68	G	qs	14.4	14.8					1
Pinoso	1	545	21-76	G	os	14.2	14.3					1
Valencian sector (Iberian Basin)	***18***							***14.5***	***15.2***	***0.3***	***1.3***	
Chelva	5	150	Ys.Ch-3	G	o	14.4	15.0	*14.7*	*15.7*	*0.3*	*1.3*	5
		325 bis	Ys.Ch-9	G	os	15.0	17.3					1
		317	Ys.Ch-23	G	os	14.9	16.6					1
		413	Ys.Ch-36	G	o	14.3	13.9					1
		479bis	Ch-40			14.8	15.9					1
Cofrentes	1	303	FE-6	G	o	15.0	16.1	*15.0*	*16.1*			1
Teresa de Cofrentes	2	397	Ay3-1	G	qs	14.3	13.4	*14.1*	*13.0*	*0.4*	*0.6*	1
		398	Ay3-2	G	qs	13.8	12.6					1
Alt Palància	4	120	YsAt-17	47	o	14.4	16.1	*14.5*	*15.8*	*0.4*	*0.6*	5
		144	YsAt-22	G	o	14.2	15.3					5
		121	YsAt-12	G	o	14.2	16.6					5
		377	Alt.8	G	o	15.1	15.2					1
Manzanera	6	166	YsMz-28	G	o	14.8	16.7	*14.5*	*15.6*	*0.6*	*0.8*	1
		167	YsMz-29	G	o	14.6	16.0					1
		106	YsMz-8	G	o	15.4	16.3					1
		108	YsMz-6	G	o	13.8	15.0					6
		109	YsMz-4	G	o	14.0	14.9					1
		130	YsMz-17	G	os	14.5	14.8					6
Catalan Basin	**16**							**14.9**	**13.9**	**0.0**	**1.3**	
A. Baix Ebre sector	***4***	431	KMI-6	G	os	14.6	13.8	***14.9***	***13.1***	***0.2***	***0.8***	1
		433	KMI-8	G	os	15.0	13.6					1
		434	KMI-9	G	os	14.8	12.3					1
		435	KMI-10	G	os	15.0	12.5					1
B. Priorat-Prades sector	***5***		K-1	G	os	14.7	15.1	***14.8***	***15.4***	***0.1***	***0.8***	4
			K-2	G	o	14.8	15.0					4
			Ga-28	G	os	15.0	16.5					4
			Ga-29	G	os	14.8	15.8					4
		416	KGA-1	G	os	14.9	14.4					1
C. Gaià-Montseny sector	***7***		ES-22	G	os	14.6	13.5	***14.9***	***13.3***	***0.5***	***0.8***	4
			ES-24	G	os	14.2	12.6					4
			Co-23	G	os	14.5	14.1					4
		441	KCO-6	G	os	15.0	13.6					1
		456	KCO-5	G	os	14.8	13.2					1
		457	KCO-7	G	os	15.3	13.9					1
		458	KCO-8	G	os	15.7	11.9					1

Lithlogy: G, gypsum; A, Anhydrite. **Occurrence of the sample:** o, outcrop; os, stratigraphic section; q, quarry; qs, quarry section; db; deep borehole. **Stdv:** standard deviation. **Ref.:** 1, This study; 4, Ortí et al., 2018; 5, Ortí et al., 2020; 6, Pérez-López et al., 2021a.

The lowest values were recorded in the Ballobar sub-basin of the Ebro basin (up to 11.5‰ in the Bujaraloz borehole, Table 7), and La Mancha sector of the Iberian basin (Carcelén borehole, 13.3‰; Fig. 7). As a whole, however, our $\delta^{34}S$ mean values for the Anhydrite Zone (~14‰) are not too different from those recorded in the Atlantic province by Holser et al. (1988). In the Grand Banks of Canada, these authors reported $\delta^{34}S$ values ranging from 12.1‰ to 14.6‰ in the Argo Formation (Hettangian-Sinemurian) and from 10.4‰ to 13.5‰ in the Iroquois Formation (Sinemurian-Aalenian?). These low values were assumed by Holser et al. (1988) as primary signatures, being more representative of marine evaporites of Early Jurassic age than those in the global $\delta^{34}S$ curve of Claypool et al. (1980). Alternatively, Holser et al. (1988) proposed that $\delta^{34}S$ values in the Atlantic province could have been lowered by local effects of volcanic or hydrothermal activity, or continental water inputs. For the 'Late Triassic' Canadian deposits of Alberta (Charlie Lake Formation), Claypool et al. (1980; their Appendix) reported a mean value of 14.2‰ and rang of 13.4‰ to 15.7‰ (9 samples, mainly of anhydrite).

Low $\delta^{34}S$ mean values ranging from ~13‰ to ~16‰ have been recorded in the 'Late Triassic' evaporites of the Western Tethys-Mediterranean area by several authors (Claypool et al., 1980; Cortecci et al., 1981; Rick, 1990; Utrilla et al., 1992; Longinelli and Flora, 2007). A volcanic influence was assumed by Boschetti et al. (2011) for these evaporites. According to Boschetti et al. (2011), the oceanic water in this area would have received supplies of ^{34}S-depleted sulfate from the oxidation of volcanogenic S-bearing volatiles with $\delta^{34}S$ values close to 0‰. This supply would be linked to coeval oceanic rifting and volcanism in the Central Atlantic Magmatic Province (CAMP).

With regard to the low $\delta^{34}S$ values recorded for the Anhydrite Zone in this study, a primary interpretation can be assumed for them. Their variability, however, could have been influenced by some factors such as volcanism, mixing with nonmarine waters in extensive lagoons, and local precipitation from brines affected by BSR action.

Table 6
Isotopic data ($\delta^{34}S$, $\delta^{18}O$) of the evaporites in the upper unit of the upper Keuper (K5) of eastern Iberia documented in this study.

Unit basin/*sector*/outcrop	n	Lab. sample no.	Field sample name	Lithology	Occurrence	$\delta^{34}S$ (‰)	$\delta^{18}O$ (‰)	Mean $\delta^{34}S$ (‰)	Mean $\delta^{18}O$ (‰)	Stdv $\delta^{34}S$ (‰)	Stdv $\delta^{18}O$ (‰)	Ref.
- Upper Keuper (K5)	**46**							**14.9**	**13.6**	**0.1**	**0.7**	
Maximum value:						16.0	19.0					
Mínimum value:						13.3	8.9					
Eastern Betic sector Prebetic zone	***12***							***14.5***	***12.5***	***0.4***	***1.7***	
La Celia	2		DLC-1	G	o	14.5	10.7	*14.6*	*10.8*	*0.1*	*0.1*	3
			DLC-2	G	o	14.6	10.8					3
Jumilla	2	391	3	G	qs	13.9	10.7	*14.0*	*11.1*	*0.2*	*0.6*	1
		392	4	G	qs	14.1	11.5					1
Los Morrones (Ontur)	3	525	21-38	G	qs	14.7	12.8	*14.3*	*13.4*	*0.5*	*1.5*	1
		528	21-41	G	qs	13.8	15.1					1
Montealegre		529	21-54	G	qs	14.3	12.3					1
Pinoso	1	546	21-77	G	os	15.1	15.0	*15.1*	*15.0*	-	-	1
Almansa	4	394	Am.4	G	os	14.3	12.0	*14.4*	*12.3*	*0.3*	*1.2*	1
		395	Am.5	G	os	14.1	12.1					1
		396	Am.6	G	os	14.3	11.1					1
Cerro Buenavista		510	21-60	G	qs	14.8	14.0					1
Valencian sector (Iberian basin)	***28***							***14.6***	***13.6***	***0.6***	***2.9***	
Carcelén-1	2		T12 1948	A	db	13.9	8.9	*13.7*	*9.0*	*0.3*	*0.1*	2
			T12 1949	A	db	13.5	9.0					2
Cofrentes	1	300	FE-8	G	os	15.6	18.5	*15.6*	*18.5*	-	-	1
Teresa de Cofrentes	4	399	Ay2-1	G	os	13.9	12.9	*14.8*	*13.6*	*0.7*	*1.7*	1
		400	Ay2-4	G	os	15.6	16.2					1
		426a	KMI-1	G	qs	14.8	12.9					1
		426b	KMI-1	G	qs	14.8	12.4					1
Chelva	3	155	Ys.Ch-6	G	os	15.5	18.0	*14.7*	*13.4*	*0.8*	*4.0*	5
		409	Ys.Ch-32	G	o	14.0	11.0					1
		411	Ys.Ch-34	G	o	14.5	11.2					1
Alt Palància	7	112	YsAtP-1	G	q	13.3	10.7	*14.1*	*12.2*	*0.4*	*1.5*	5
		136	YsAtP-2	G	q	13.9	10.4					5
		100	ZA-Anh.	G	o	14.3	11.6					5
		103	YP.ZA-1	G	o	14.0	11.2					5
		134	YP.ZA-2	G	o	14.1	12.4					5
		375	Alt-6	G	q	14.8	15.0					1
		381	Alt-12	G	qs	14.5	12.5					1
		478	Alt-23	G	qs	14.0	13.4					1
Manzanera	8	157	YsMz-18	G	qs	15.1	12.3	*14.6*	*14.8*	*0.4*	*2.1*	6
		131	YsMz-19	G	qs	14.9	13.0					6
		111	Ys SCM-1	G	q	14.8	16.3					1
		177	YsSCM-2	G	q	14.4	14.8					1
		178	YsSCM-3	G	q	14.3	15.0					1
		179	YsSCM-4	G	q	14.2	15.0					1
		180	YsSCM-5	G	q	14.2	19.0					1
		308	YsSCM-6	G	q	14.7	13.2					1
Villahermosa	3	122	Ys.Vll-1	G	q	14.4	12.0	*14.8*	*13.5*	*0.5*	*1.4*	1
		147	YsVll-2	G	q	14.6	13.6					1
		169	Ys.Vll-3	G	q	15.3	14.8					1
Catalan basin	**6**							**15.6**	**14.7**	**0.3**	**1.2**	
	6		Ga-8	G	os	15.3	16.5					4
		417	KGA-2	G	os	15.0	13.6					1
		419	KGA-4	G	os	15.4	14.1					1
		420	KGA-5	G	os	15.8	13.8					1
		421	KGA-6	G	os	15.6	14.6					1
		422	KGA-7	G	os	16.0	15.7					1
		423	KGA-8	G	os	15.8	16.3					1

Lithlogy: G, gypsum; A, Anhydrite. **Occurrence of the sample:** o, outcrop; os, stratigraphic section; q, quarry; qs, quarry section; db; deep borehole. **Stdv:** standard deviation. **Ref.:** 1, This study; 2, Utrilla et al., 1992; 3, Ortí et al., 2014; 4, Ortí et al., 2018; 5, Ortí et al., 2020; 6, Pérez-López et al., 2021a.

7. Comparison with the Triassic successions of Central-Southern Europe

7.1. Isotope values for the Germanic basin

Bernasconi et al. (2017) reported $\delta^{34}S$ isotope data for Middle-Upper Triassic Ca-sulfates in Northern Switzerland (Jura Mountains) obtained through exhaustive sampling in boreholes (anhydrite) and on the surface (gypsum; Riepel outcrop) (Table 8). These evaporites represent epicontinental platform deposits (shallow marine and coast areas) at the southern margin of the intracratonic Germanic basin. At this margin, the Triassic units richest in evaporites are intercalated within the sediments of the Middle Muschelkalk (Sulfatschichten unit of the Anhydritgruppe) and Middle Keuper (Gipskeuper unit). Other Triassic units, although predominantly calcareous, also bear variable amounts of Ca-sulfates in the subsurface mainly as anhydrite nodules (Fig. 12).

The following findings by Bernasconi et al. (2017) are of interest for the present study: (i) in the time interval between the Anisian and the Julian (early Carnian), $\delta^{34}S$ values show a marked decrease from the Röt unit (from ~24‰ to ~22‰) to the top of the Gipskeuper unit (~15.5‰). The change to slightly increasing values is detected at the base of the Upper Keuper (Gansingen Dolomite; Tuvalian, late Carnian)

Table 7
Isotopic data ($\delta^{34}S$, $\delta^{18}O$) of the evaporites in the Anhydrite Zone (Rhaetian-Hettangian-Sinemurian) and interbedded in the carbonates of the Zamoranos Formation (Rhaetian) and the Early Jurassic carbonates (Sinemurian-Pliensbachian) of eastern Iberia documented in this study.

Unit basin/*sector*/outcrop	n	Lab sample no.	Field sample name	Lithology	Occurrence	$\delta^{34}S$ (‰)	$\delta^{18}O$ (‰)	Mean $\delta^{34}S$ (‰)	Mean $\delta^{18}O$ (‰)	Stdv $\delta^{34}S$ (‰)	Stdv $\delta^{18}O$ (‰)	Ref.
- Clayey anhydritic Limestone	**2**							**19.1**	**11.7**	**0.2**	**0.8**	
Maximum value:						19.2	12.3					
Minimum value:						18.9	11.1					
Valencian sector (I.b.)	***2***							***19.1***	***11.7***	***0.2***	***0.8***	
Carcelén-1	2		T5 1015 m	A	sb	19.2	12.3					2
			T5 1018 m	A	sb	18.9	11.1					2
- Dolostone with gypsum	**2**							**16.4**	**14.6**	**0.1**	**0.2**	
Maximum value:						16.4	14.7					
Minimum value:						16.3	14.4					
Eastern Betic sector (Prebetic)								***16.4***	***14.6***	***0.1***	***0.2***	
Cerro Madroño (On.)	2	518	21-31	G	os	16.4	14.7					1
		521	21-34	G	os	16.3	14.4					1
- Anhydrite zone (AZ)	**35**							**14.2**	**13.8**	**1.2**	**3.8**	
Maximum value:						16.3	19.6					
Minimum value:						11.5	9.4					
Eastern Betic sector (Prebetic)	***2***							**15.3**	**19.5**	**0.1**	**0.1**	
Morrones Albatana (On.)	2	523	21-36	G	qs	15.4	19.6					1
		524	21-37	G	qs	15.2	19.4					1
Valencian sector (I.b.)	***11***							***14.5***	***11.5***	***0.6***	***2.0***	
Carcelén-1 (borehole)	4		T9 1242m	A	db	16.3	12.6	*14.8*	*11.6*	*1.2*	*2.0*	2
			T9 1247m	A	db	14.8	13.9					2
			T11 1522m	A	db	14.8	9.7					2
			T11 1525m	A	db	13.3	10.2					2
Perenchiza (borehole)	1		2350m	A	db	13.8	9.4	*13.8*	*9.4*	-	-	2
Chelva	6	151	Ys.Ch-5	G	os	15.0	11.5	*14.8*	*13.4*	*0.3*	*1.8*	5
		326	Ys.Ch-10	G	os	14.9	16.8					1
		327	Ys.Ch-11	G	os	14.8	13.0					1
		489	Ch-51	G	os	14.6	12.8					1
		491	Ch-53	G	os	15.2	12.6					1
		492	Ch-54	G	os	14.4	13.5					1
Aragonian branch (I.b.)	***16***							***14.5***	***11.7***	***0.0***	***0.4***	
Alacón (borehole)	10	3	3-801 m	A	sb	14.4	11.0	*14.5*	*11.4*	*0.4*	*0.5*	1
		9	9-783 m	A	sb	14.2	11.0					1
		19	19-752 m	A	sb	14.3	10.8					1
		27	27-724.70	A	sb	14.2	11.1					1
		39	39-697.60	A	sb	14.2	11.7					1
		50	50-671.10	A	sb	14.6	11.5					1
		66	66-642.30	A	sb	14.3	11.2					1
		79	79-620.70	A	sb	14.5	11.6					1
		91	91-599.60	A	sb	14.5	11.6					1
		124	124-495.8	A	sb	15.5	12.7					1
Ezcaray (borehole)	6	359	~287 m	A	sb	14.6	12.4	*14.5*	*12.0*	*0.2*	*0.7*	1
		360	257 m	A	sb	14.8	11.7					1
		361	229 m	A	sb	14.5	11.8					1
		362	211 m	A	sb	14.2	11.6					1
		363	190 m	A	sb	14.5	11.2					1
		364	172 m	A	sb	14.2	13.2					1
Ebro basin (I.b.)	***6***							***12.4***	***12.6***	***0.9***	***0.8***	
La Zaida	3		556 m	A	db	14.5	12.2	*13.4*	*11.9*	*0.9*	*0.9*	2
			696 m	A	db	12.9	12.6					2
			839 m	A	db	12.9	10.9					2
Bujaraloz	2		1460 m	A	db	11.5	12.5	*11.9*	*12.5*	*0.5*	*0.1*	2
			1605 m	A	db	12.2	12.4					2
Monegrillo	1		889 m	A	db	11.9	13.5	*11.9*	*13.5*	-	-	2
- Zamoranos Fm	**3**							**16.4**	**13.3**	**0.1**	**0.7**	
Maximum value:						16.5	13.8					
Minimum value:						16.1	12.7					
Eastern betic sector	***3***							***16.4***	***13.3***	***0.1***	***0.7***	
Calasparra (Subbetic)	1	569	21F-Y39	G	*os*	16.4	13.8					1
Almansa (Prebetic)	2	509	21-23	G	*os*	16.5	12.7	*16.3*	*12.8*	*0.3*	*0.1*	1
		513	21-65	G	*qs*	16.1	12.8					1

Lithlogy: G, gypsum; A, Anhydrite. **Occurrence of the sample*:*** o, outcrop; os, stratigraphic section; q, quarry; qs, quarry section; db; deep borehole. **Stdv:** standard deviation**. Ref.:** 1, This study; 2, Utrilla et al., 1992. ***I.b.***: Iberian basin; On.: Ontur locality.

with $\delta^{34}S$ mean values of 16.4‰ recorded in anhydrite samples and 15.7‰ in gypsum samples; (ii) in the Gipskeuper unit, two timing interpretations are proposed for the maximum evaporite precipitation. In interpretation I, this occurred in the Longobardian (late Ladinian) and in interpretation II in the Julian (early Carnian); and (iii) both the Sulfatschichten and the Gipskeuper units show similar decreasing $\delta^{34}S$

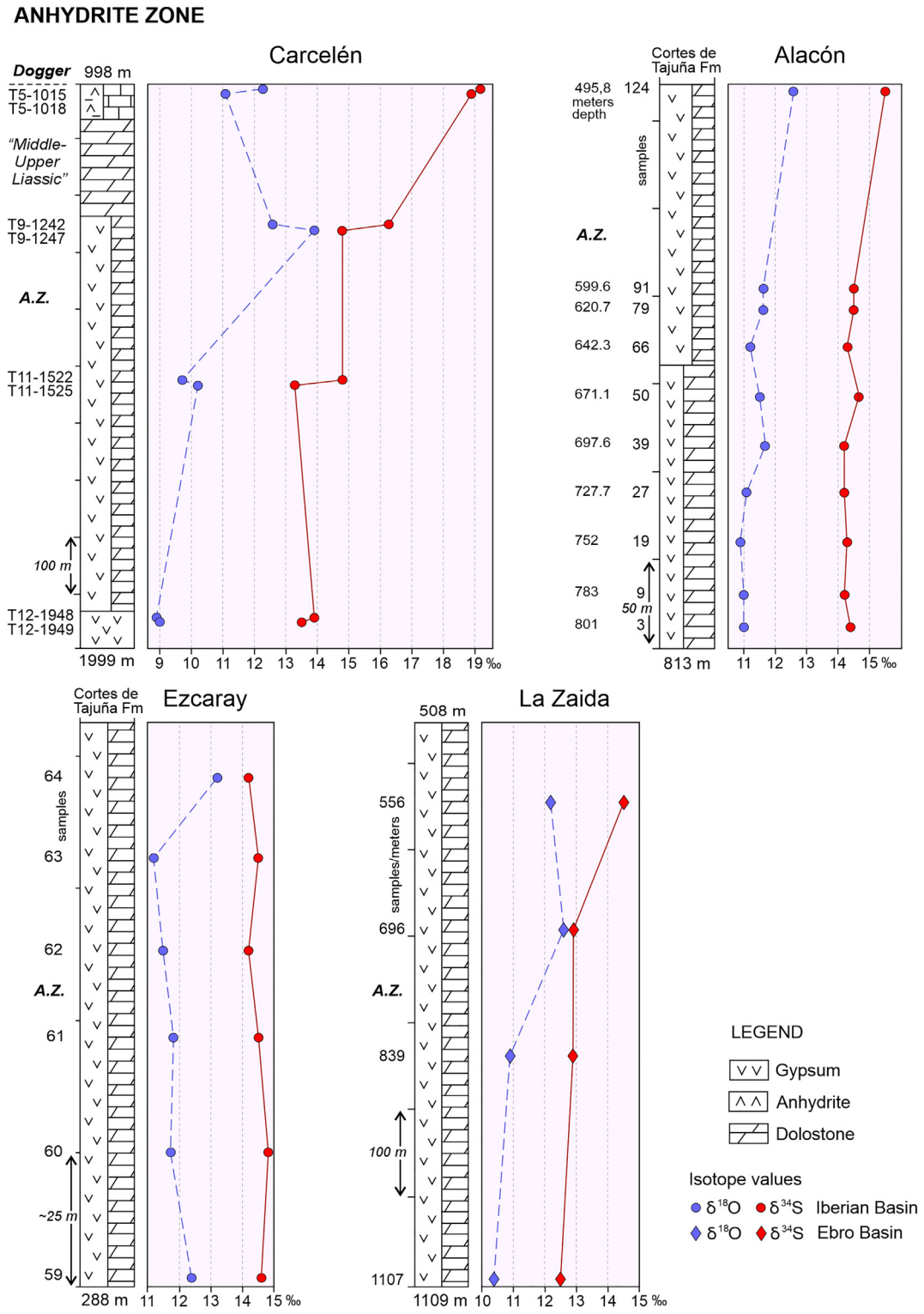

Fig. 7. Isotope profiles ($\delta^{34}S$, $\delta^{18}O$) of the Anhydrite Zone (Rhaetian-Hettangian) in some boreholes. The stratigraphic location of the samples is indicated. Deep (oil) boreholes: Carcelén-1 (La Mancha sector, Iberian basin) and La Zaida-1 (Ebro basin). Boreholes (shallower) for hydrogeologic prospection: Alacón (Teruel province) and Ezcaray (La Rioja) in the Aragonian Branch of the Iberian basin.

trends from base to top with ~3‰ of scatter. For the two evaporite units, differences of 1‰ or 2‰ were observed in samples from different boreholes despite their geographical proximity.

Also in Northern Switzerland, $\delta^{34}S$ data for the Gipskeuper unit had been formerly supplied by Rick (1990), who obtained a mean value of 16.5‰, and by Pearson et al. (1991), who reported a mean value of 14.6‰ (quoted in Table 2 of Boschetti et al., 2011). For the equivalent unit of the Gipskeuper in Lorraine (France), i.e. the 'Marnes irisées inférieures' of Geisler et al. (1978), a mean value of 15.5±0.4‰ was provided by Fanlo and Ayora (1998) (Table 8).

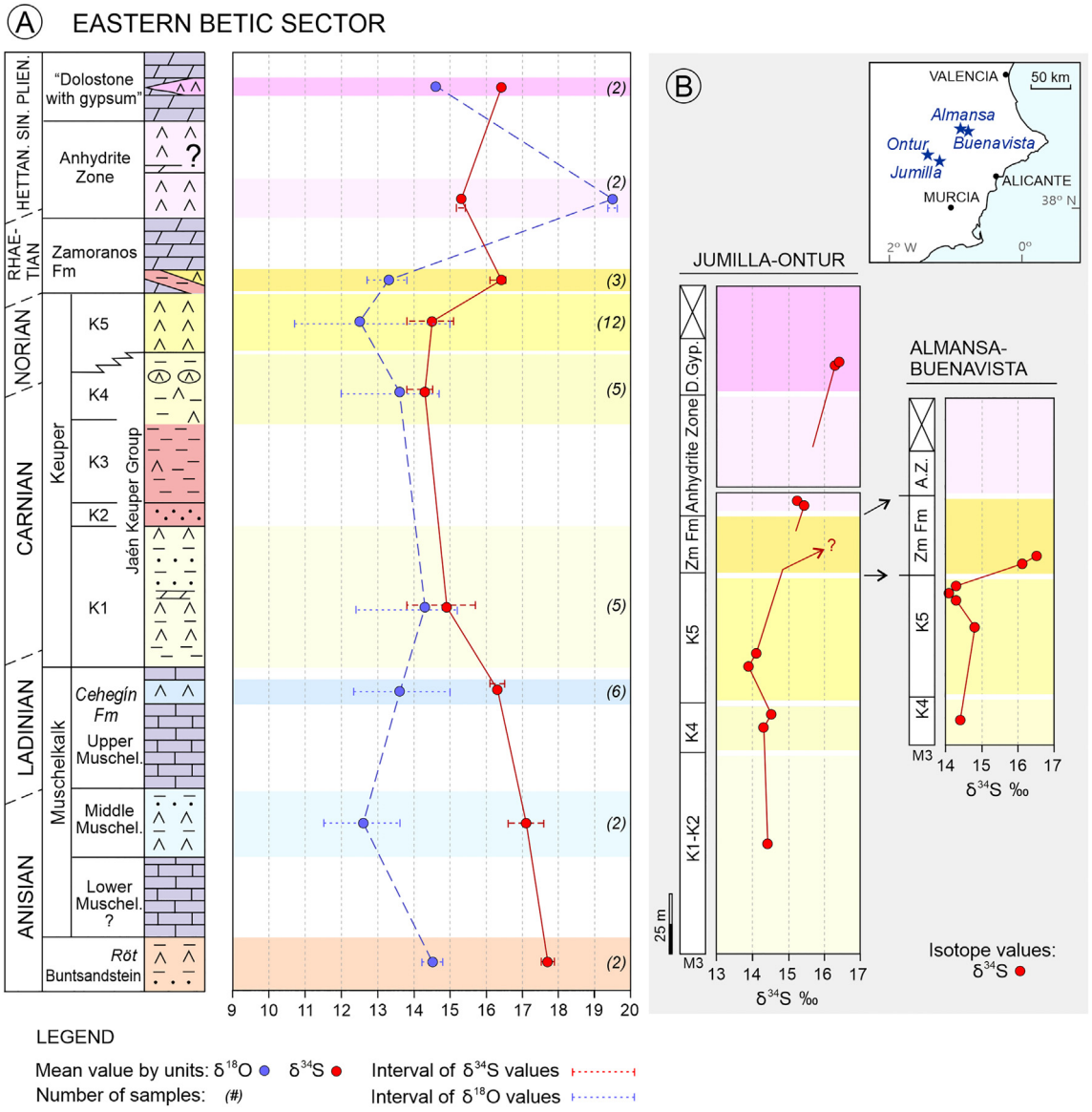

Fig. 8. (A). Isotope trends of mean values ($\delta^{18}O$, blue discontinuous line; $\delta^{34}S$, red continuous line) of the evaporite units in the eastern Betic sector. The range of individual values (discontinuous horizontal lines) is indicated. (B) Isotope $\delta^{34}S$ trends of two representative sections in the eastern Betic sector.

With regards to the $\delta^{18}O$ values for the Middle-Upper Triassic evaporites in the Germanic basin, scarce data were found. The Gipskeuper samples studied by Rick (1990) yielded $\delta^{18}O$ values in the range 11.20‰ to 12.79‰ (mean value of 11.3 ± 1.7‰), and those examined by Pearson et al. (1991) yielded a $\delta^{18}O$ mean value of 13.2 ± 0.8‰. The samples studied by Fanlo and Ayora (1998) in Lorraine showed a $\delta^{18}O$ mean value of 13.0‰ ± 1.1‰, ranging from 11.2‰ to 14.1‰.

Precise correlation between the evaporites of the Northern Switzerland sector of the Germanic basin and the corresponding units in the Triassic basins of eastern Iberia is not yet possible because of the lack of accurate dating for the Iberian units, which is limited to palynological determinations. This means the stratigraphic correlation here assumed is tentative (Table 8). In the two Triassic domains, a continuous decreasing trend for $\delta^{34}S$ values was recorded from the Röt and the middle Muschelkalk units (Anisian) to the top of the upper Keuper (Norian). However, the mean values obtained in the units of eastern Iberia, which decreased from ~17.7‰ in the Röt unit to 14.9‰ at the top of the upper Keuper (K5 unit), were lower than in the Germanic basin. The $\delta^{18}O$ mean values in the Keuper units of eastern Iberia (Fig. 4) are slightly higher than those reported by Rick (1990) and Pearson et al. (1991) for the Gipskeuper of the Germanic basin (see above).

7.2. Isotope values in the Alp-Apennine domains

Bernasconi et al. (2017) also compiled isotope data on evaporite units of the Permian-Triassic basins in the Alp and Apennine chains (Cortecci et al., 1981; Spötl and Pak, 1996; Kampschulte et al., 1998; Longinelli and Flora, 2007; Boschetti et al., 2011). In Austria and Italy, these evaporites reflect marine shelf-to-basin settings open to the Tethys. Additionally, Bernasconi et al. (2017) provided new $\delta^{34}S$ data for the Carniola di Bovegno in the Southern Alps (Lombardy), of lowest Anisian age, and for the Raibler Formation in the Northern Calcareous Alps (Lech, in Austria), of Norian or Norian-Rhaetian age. The $\delta^{34}S$ trends proposed by Bernasconi et al. (2017) in these domains for the Early-Late Triassic are summarized in Supplementary Data (Table 3S).

For the Anisian evaporites of the Carniola di Bovegno, Cortecci et al. (1981) obtained two $\delta^{34}S$ values (16.9‰, 17.2‰), which are almost

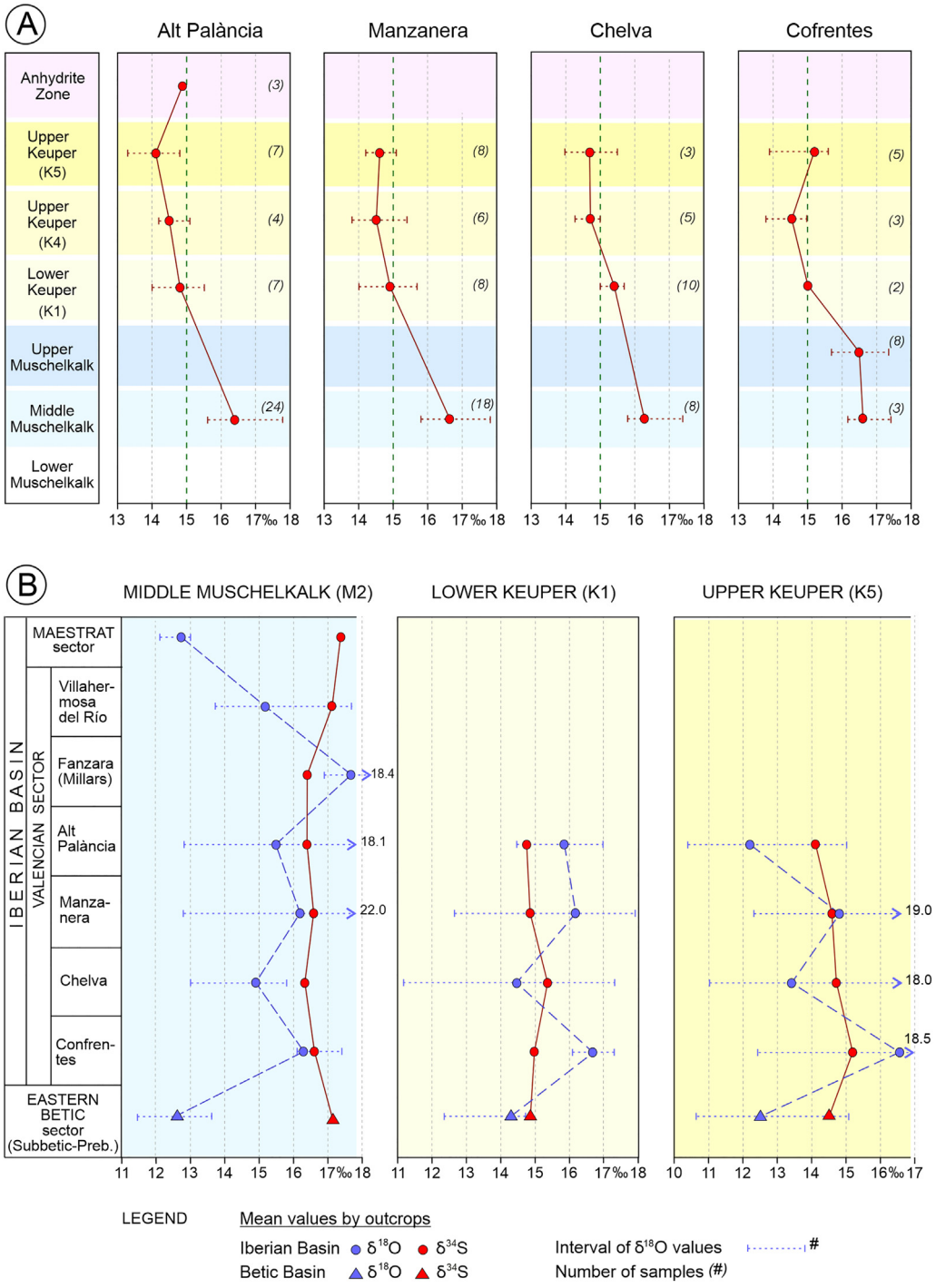

Fig. 9. (A) Isotope trends of $\delta^{34}S$ mean values recorded for several outcrops of the Valencian sector of the Iberian basin. (B) Isotope trends of $\delta^{34}S$ and $\delta^{18}O$ mean values for several evaporite units in the eastern Betic sector and in the Valencian and Maestrat sectors of the Iberian basin. Note the variability of the $\delta^{18}O$ mean values and the large scatter of the individual samples (discontinuous horizontal lines).

identical to the six determinations ranging from 16.9‰ to 17.2‰ more recently obtained by Bernasconi et al. (2017; their Appendix). For the Carnian evaporites of the Austrian Eastern Alps, Götzinger et al. (2001) reported $\delta^{34}S$ values ranging from 14‰ to 16‰, with a mean value of 15.8 ± 0.4‰ (data quoted in Schroll and Rantitsch, 2005). Further, for marine barite samples also from the Eastern Alps in Austria, a $\delta^{34}S$ mean value of 14.6 ± 1‰ was reported by Schroll et al. (1983). In the upper Carnian (Tuvalian) evaporites of the Raibler Formation (Lech, Austria; Northern Calcareous Alps), the isotope analyses by Bernasconi et al. (2017) yielded $\delta^{34}S$ values from 16.3‰ to 17.7‰, with mean value of 17.1‰ (n = 11). In the 'Late Triassic' evaporites of the Alp-Apennine domains, Cortecci et al. (1981) obtained the following $\delta^{34}S$ ranges: 16.5‰ to 17.4‰ (n = 5) for the upper Carnian (Southern Alps); 15.8‰ to 16.9‰ for the 'Late Trias' (Central and Western Alps); and 15.0‰ to 17.4‰ for the Norian-Rhaetian Burano Formation (Adriatic Evaporitic Area of the Apennines).

The Burano Formation is comprised of large volumes of metamorphosed evaporites located at the base of structural, thrusted units. The

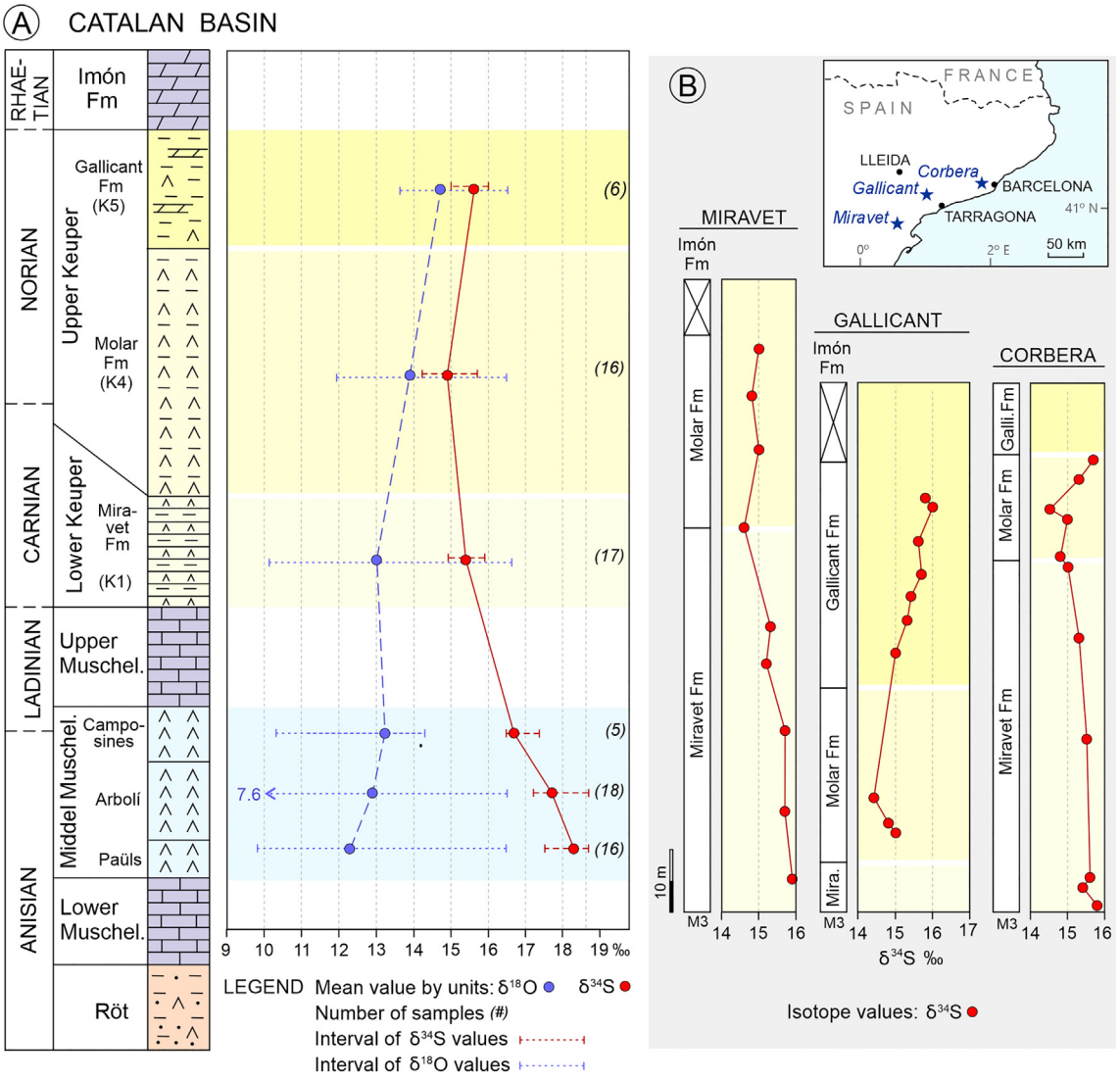

Fig. 10. (A) Isotope trends of $\delta^{34}S$ and $\delta^{18}O$ mean values of the evaporite units in the Catalan basin ($\delta^{18}O$, blue discontinuous line; $\delta^{34}S$, red continuous line). (B) $\delta^{34}S$ profiles in some representative sections are shown.

$\delta^{34}S$ analyses obtained for this unit by Boschetti et al. (2011) in the Northern Apennines range from 15.1‰ to 16.0‰, with a mean value of 15.5 ± 0.4‰ (n = 8). Boschetti et al. (2011) also compiled data for this unit along the Apennine chain, and obtained a $\delta^{34}S$ mean value of 15.2 ± 0.2‰ (n = 38) for all these Apennine evaporites after eliminating some high values considered to be outliers (including two values of 17.0‰ and 17.4‰ described by Cortecci et al., 1981, for the Peruggia-2 borehole in Umbria).

When comparing all literature $\delta^{34}S$ data for the Alp-Apennine domains with those obtained by us in eastern Iberia, the following observations should be highlighted. For the Anisian evaporites, similar values are observed in the Carniola di Bovegno Formation of the southern Alp domain (~17‰) and in eastern Iberia (mean value of 17.7 ± 0.3‰ for the Röt unit and 17.2 ± 0.5‰ for the middle Muschelkalk unit). For the 'Late Triassic', the majority of $\delta^{34}S$ values for the Alp-Apennine domains, in the range ~17.5‰ to ~15.5‰, are ~2‰ higher than those reported in eastern Iberia for the Carnian-Norian, ranging from ~14.5‰ to ~15.5‰. Only the values considered to be primary signals by Boschetti et al. (2011) in the Burano Formation across the Apennines ($\delta^{34}S$ mean value of 15.02 ± 0.2‰) are comparable to those in the upper unit of the upper Keuper (K5; $\delta^{34}S$ mean value of 14.9 ± 0.1‰) in eastern Iberia. Because of the respective stratigraphic/isotopic characteristics, similarities between the Burano Formation and the K5 unit (Ayora Formation; Ortí, 1974) seem to exist.

For the Alp-Apennine domains, $\delta^{18}O$ values widely range from ~10‰ to ~18‰. However, most common values fall within the range ~10.5‰ to ~12.5‰ (Cortecci et al., 1981; Boschetti et al., 2011). Based on these $\delta^{18}O$ data, Boschetti et al. (2011) distinguished two main groups of evaporite units in the Upper Triassic of the Western Tethys (Supplementary Data, Table 4S). One most abundant group is comprised of units that feature relatively low values of ~9‰ to ~14‰, which are considered primary signals. The evaporites of the other group display higher $\delta^{18}O$ mean values and wider scatter of values as in the Alp-Apennine domains, being also high the corresponding $\delta^{34}S$ values. Boschetti et al. (2011; their Fig. 3A) interpreted this second group as 'secondary sulfates' and assigned the concomitant changes produced in their $\delta^{34}S$ and $\delta^{18}O$ values to bacterial sulfate reduction or to metamorphism,

7.3. Differences and affinities in the $\delta^{34}S$ values

A new global $\delta^{34}S$ age curve for the Latest Permian (Lopingian)-Late Triassic (Norian) time interval has been proposed by Bernasconi et al. (2017) (Fig. 12). The curve is based on the extensive data compiled by

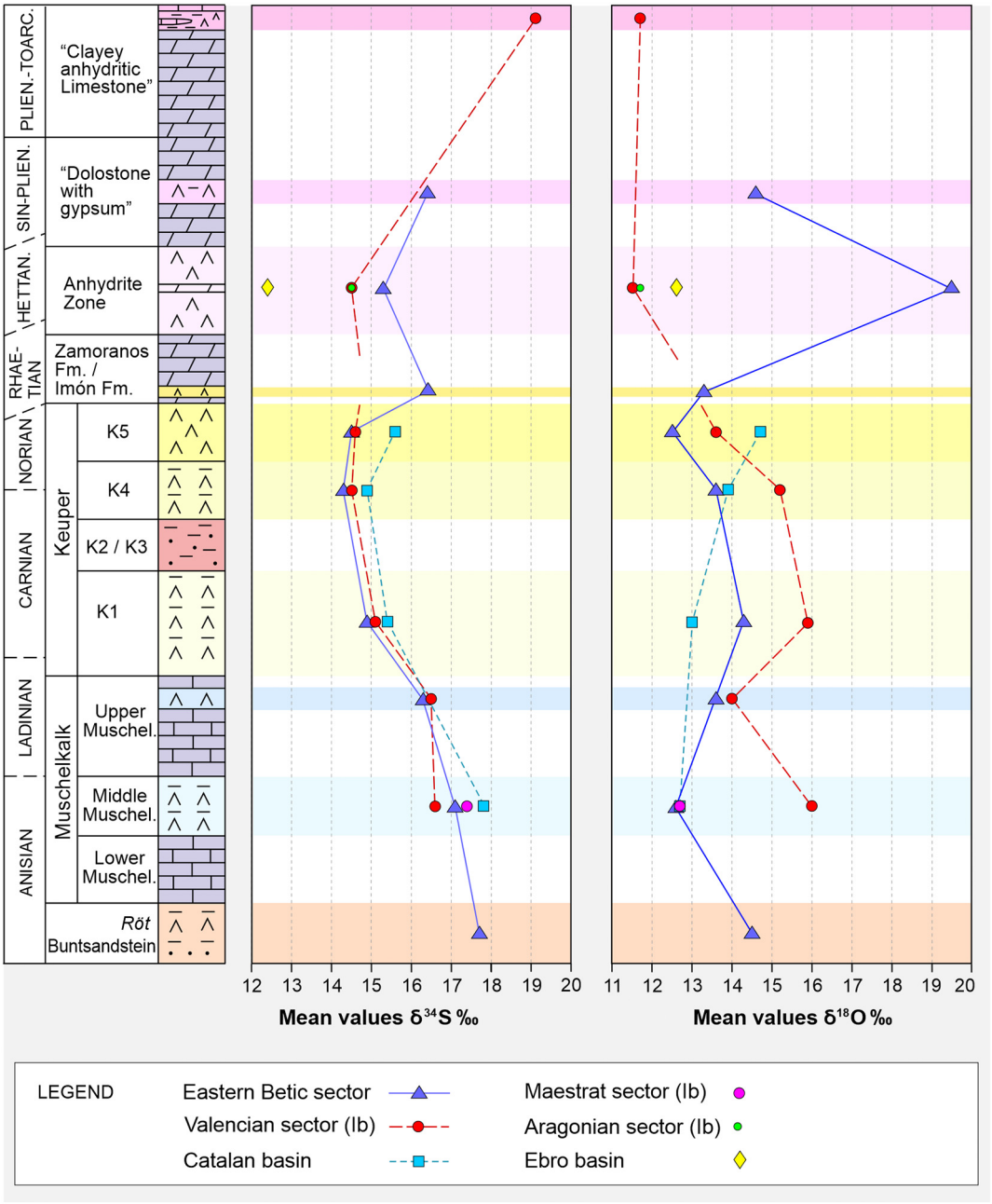

Fig. 11. Isotopic trends of $\delta^{34}S$ and $\delta^{18}O$ mean values of the evaporite units in the eastern Betic sector, the Catalan basin, and the Valencian sector of the Iberian basin (Ib). The projection of some isolated mean values refers to the Anhydrite Zone in the Ebro basin and the Aragonian sector of the Iberian basin, and to the middle Muschelkalk in the Maestrat sector of the Iberian basin (Ib). The high $\delta^{18}O$ mean value of the Anhydrite Zone in the eastern Betic sector corresponds two samples with probably anomalous values (Fig. 4, Table 7).

these authors and on the newest radiometric absolute age scale provided in the literature (Furin et al., 2006; Brack et al., 2007; Mundil et al., 2010; Mietto et al., 2012; and Wotzlaw et al., 2014 for the Middle-Late Triassic). This new scale, estimated to be of sub-million year resolution, is held as most representative of the $\delta^{34}S$ changes experienced by dissolved sulfate in the coeval marine waters of the western Tethys realm.

As stated above, a major difference between the global $\delta^{34}S$ curve by Bernasconi et al. (2017) and the data in the present study for the Middle-Late Triassic evaporites is the lower values recorded in eastern Iberia, ~1‰ to ~3‰ or even more depending on the units (Fig. 12). No clear explanation can be proposed here for this, except insufficient sampling for some units in our study. Although very scarce, our values for the lower Anisian (Röt unit) are similar only to those of the Carniola di Bovegno (Southern Alps; CB in Fig. 12; probably of Olenekian-Anisian transition or earliest Anisian age). For the upper Anisian (Illyrian), our values (middle Muschelkalk unit) are still lower than those of the global $\delta^{34}S$ curve provided by Bernasconi et al. (2017). And for the upper Carnian-Norian interval, $\delta^{34}S$ values in eastern Iberia are somewhat lighter also, mostly in the range ~14.5‰ to ~15.5‰ for the K4 and K5 units.

Considering the $\delta^{34}S$ values in the Canadian 'Late Triassic' deposits by Claypool et al. (1980) and Hettangian-Sinemurian by Holser et al. (1988), and those formerly supplied in the Late Triassic of eastern Iberia by Utrilla et al. (1992), Boschetti et al. (2011) highlighted a possible switch in the $\delta^{34}S$ values of the Late Triassic evaporites to regional scale. One type of evaporites corresponds to the Neo-Tethys ('Western Tethys-Mediterranean'), with $\delta^{34}S$ mean values ranging from ~13‰ to

Table 8
Comparison between the $\delta^{34}S$ (‰) values in the Middle-Upper Triassic evaporite units in the southern margin of the Germanic Basin (Northern Switzerland, Jura Mountains) according to Bernasconi et al. (2017), and the corresponding units in eastern Iberia reported in this study.

Unit (germanic units)	Germanic basin	Eastern Iberian basins
Upper Keuper	- Gansingen Dolomit (at the base of the Upper Keuper): anhydrite averaging 16.4‰ (in fenestral porosity in the Benken borehole) and gypsum averaging 15.7‰ (Siblingen borehole)	- K5 unit: values between 13.3‰ and 16.0‰, averaging 14.9‰ (n: 46) - K4 unit: values between 13.8‰ and 15.7‰, averaging 14.6‰ (n: 39)
Middle Keuper	- Gipskeuper, with five sub-units, all bearing evaporites with decreasing isotopic trend (from 17.9‰ at the base to 15.0‰ at the top of the sub-unit II, the 'Zyklische Serie' which is the richest in gypsum); the vertical scatter in the sub-units is up to ~3‰, which could also reflect variable precipitation conditions in a continental sabkha (similarly to the Sulfatschichten); the top of the Gipskeuper shows a slight increase to 15.5‰. Main set of data are found in the Weiach borehole, where values of ~16‰ are predominant towards the base and ~15‰ in the central and upper parts; in the gypsum of the Riedel outcrop, the predominant values range from ~15.5‰ to ~16.5‰. Other $\delta^{34}S$ values according to other authors: Rick (1990): mean value 16.5‰ (n: 6) (outcrop samples in the Folded Jura; Gipskeuper); Pearson et al. (1991): mean value 14.6‰ (n: 5) (borehole samples in the Tabular Jura; Gipskeuper); Fanlo and Ayora (1998): mean value 15.5 ±0.4‰ (n: 21), ranging from 14.8‰ to 15.9‰, with a single value of 16.5‰ at the base of the N unit; anhydrite samples associated with halite ('Marnes irisées inférieures'; Lorraine). - Schilfsandstein Fm, with anhydrite nodules averaging ~15‰	- Middle Keuper: siliciclastic assemblage comprised of the K2 unit, or Manuel Formation (equivalent to the Schielfsandsatein Formation, as early correlated in Ortí, 1974, Fig. 11), and the K3 unit (Cofrentes Formation), the two units bearing scarce evaporites; no isotope data are available. - Lower Keuper (K1 unit; equivalent to the Gipskeuper): values between 13.8‰ and 15.9‰, averaging 15.1‰ (n: 51)
Lower Keuper	- Lettenkohle: anhydrite nodules averaging ~16‰	- No equivalent unit has been identified in eastern Iberia
Upper Muschelkalk	- Trigonodous Dolomit (Fassanian): anhydrite nodules at the top; values between 19‰ and 18‰	- Uppermost part op of the upper Muschelkalk unit (top of the Royuela Formation): values between 15.7‰ and 17.4‰, averaging 16.4‰ (n: 14)
Middle Muschelkalk	- Sulfatschichten of the Anhydritgruppe: five cycles of evaporites with values between 22‰ and 19‰ averaging ~20‰; scatter of ~2 or ~3‰ from base to top in the cycles, with the higher values at the base and the lower values at the top (increased salinity from pond setting at the base, to sabkha setting at the top, according to Dronkert, 1987). - Dolomit unit: sulfates: ~20‰ - Hauptmuschelkalk: sulfates at the base (values not specified)	- Values between 15.6‰ and 18.8‰, averaging 17.2‰ (n: 107)
Top of the lower Muschelkalk	- Base of the Orbicularis-Mergel: sulfate-bearing nodules at the base of this unit with values between 24‰ and 22‰	- No equivalent unit is known in eastern Iberia
Top of the Buntsandstein (Röt)	- Anhydrite nodules: values between 23.9‰ and 17.8‰, being most representative those between 22.5‰ and 21.0‰	- Gypsum nodules: values of 17.9 and 17.5‰ (n: 2)

(n: #), number of samples in eastern Iberian documented in this study.

~16‰ (data in Claypool et al., 1980; Cortecci et al., 1981; Rick, 1990; Utrilla et al., 1992; Longinelli and Flora, 2007; Boschetti et al., 2011). The other type refers to the Eastern Paleo-Tethys ('Eastern Tethys-Mediterranean?'), with $\delta^{34}S$ samples values ranging from ~16‰ to ~19‰ (data in Claypool et al., 1980; Kampschulte and Strauss, 2004; Gündoğan et al., 2008). Our $\delta^{34}S$ values in eastern Iberia clearly correspond to the 'Western Tethys-Mediterranean' type of evaporites of Boschetti et al. (2011), and relationships seem to exist between the Canadian and the eastern Iberian values for the Hettangian-Sinemurian time interval.

8. Conclusions

In this study, the isotope compilation was not exhaustive and sampling sites were irregularly distributed both regionally and stratigraphically. Thus, future additions and corrections will be needed to gain a more comprehensive understanding of this complex subject. Despite this, the $\delta^{34}S$ and $\delta^{18}O$ datasets that characterize isotopically the evaporite units accumulated in eastern Iberia during the Middle Triassic to Early Jurassic allow for a first comparison with well-established isotope compositions in the coeval basins of Central-Southern Europe (Germanic basin, Alp-Apennine domains).

$\delta^{34}S$ values for eastern Iberia are rather homogeneous in basins, basin sectors, and outcrops and are considered primary isotope signatures. Small $\delta^{34}S$ differences in specific units detected between the basins could be assigned to local conditions of precipitation or small diachronism. By evaporite units, $\delta^{34}S$ mean values show the following trends: a continuous decrease from the Röt unit of the lower Anisian (~18‰) to the upper Keuper units of the Carnian-Norian (~15‰); an increase in the evaporite beds intercalated at the base of the Zamoranos Formation of the Rhaetian (~16‰); a decrease in the Anhydrite Zone of the Rhaetian-Hettangian-Sinemurian (~14‰; although with variable values by basin); and finally an increasing trend in the evaporite beds intercalated in the carbonates of the Sinemurian-Pliensbachian (~16‰) and the Pliensbachian-Toarcian (~19‰).

Some differences appear, however, when comparing these values with those reported for the Germanic basin and the Alp-Apennine domains. $\delta^{34}S$ mean values by units in eastern Iberia are lighter than those of their coeval evaporite units in Central-Southern Europe. Differences are greater for the Anisian (~2‰ to ~3‰) but smaller for the Ladinian-Carnian (~1.0‰ or ~1.5‰). For the Carnian-Norian, $\delta^{34}S$ mean values recorded in eastern Iberia are also lighter (~1‰ or ~2‰) than in the evaporite units of the Alp-Apennine domains. The lowest $\delta^{34}S$ mean value in the eastern Iberian units (~14‰) was recorded for the Hettangian. The change to the heavier $\delta^{34}S$ values of the Jurassic sulfates was recorded during the Sinemurian-Pliensbachian (mean value ~16.0‰) and continued in the Pliensbachian-Toarcian (mean value up to ~19‰).

Features of particular interest regarding the $\delta^{34}S$ values recorded in the evaporites of eastern Iberia are (i) the low values for the Anisian in comparison with those in the Germanic basin; (ii) after the Norian, the brief excursion to heavier values in the Rhaetian, which is here reported for the first time; (iii) the low values for several Rhaetian-Hettangian-Sinemurian successions, which are similar to those in the coeval anhydrite units of the Canadian domain.

Widely scattered $\delta^{18}O$ values were found for the majority of the evaporite units in eastern Iberia, where $\delta^{18}O$ mean values ranged from ~13.0‰ to ~14.5‰. Locally, however, these values can be higher, as recorded in some outcrops of the Valencian sector of the Iberian basin, whose $\delta^{18}O$ mean values range from ~15‰ to ~16‰.

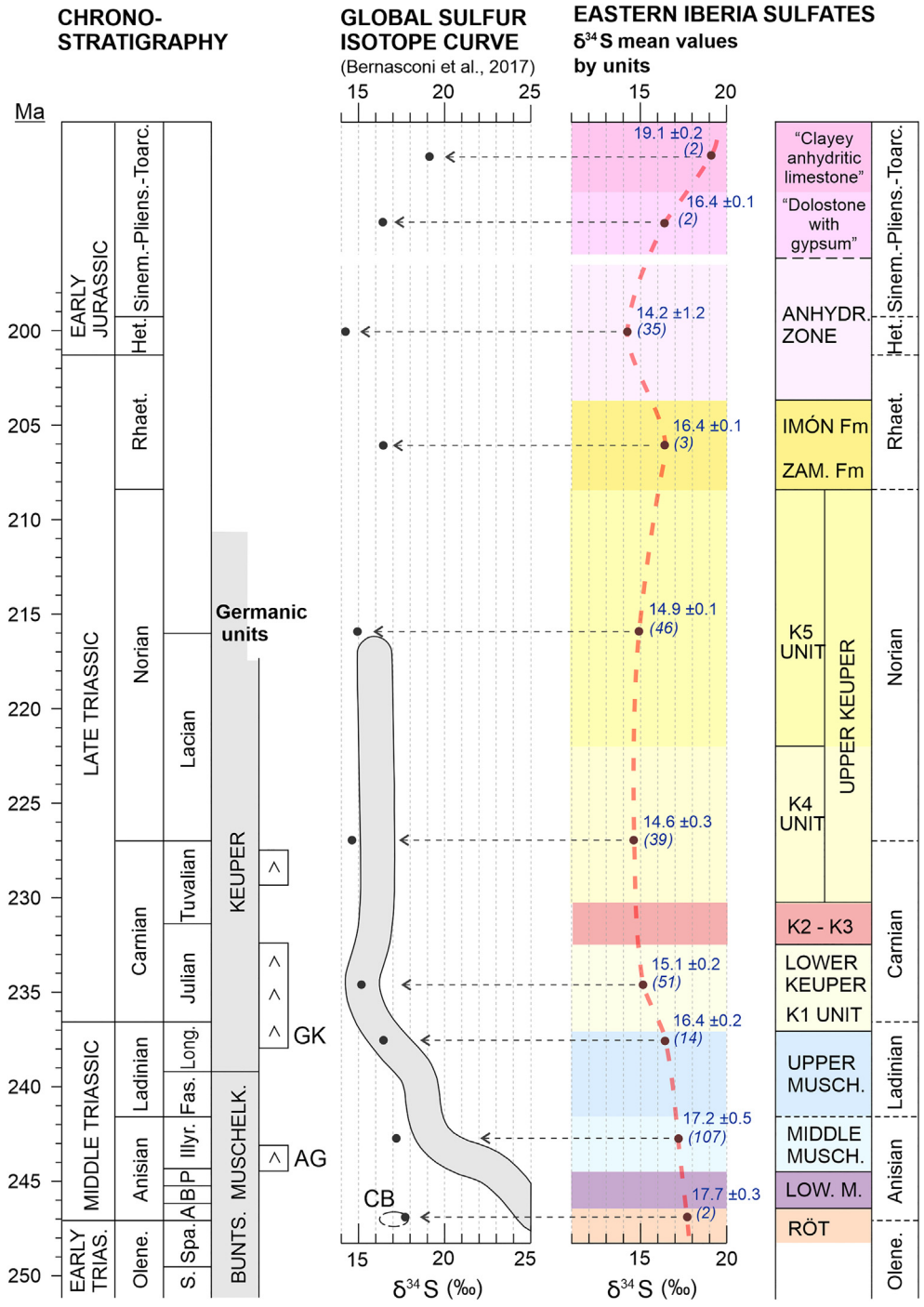

Fig. 12. Comparison between the global $\delta^{34}S$ curve for the Middle-Upper Triassic in the Germanic Basin and the Alp-Apennine domains after Bernasconi et al. (2017), and the trend of $\delta^{34}S$ mean values by evaporite units obtained in this study for eastern Iberia. For eastern Iberia, the number of samples analyzed for each unit together with the standard deviation is indicated in brackets. The global sulfur curve here was largely simplified from Fig. 5 of Bernasconi et al. (2017) and in it the shift to the Carniola di Bovegno values (CB) was not represented. The global curve by Bernasconi et al. (2017) is based mainly on the following data: The new values obtained by Bernasconi et al. (2017) in the Germanic basin for the Anisian to lower Carnian (Julian) interval (Table 8); and the new values obtained by those authors but including also values from the literature (mainly from Cortecci et al., 1981 and Longinelli and Flora, 2007) for the upper Carnian (Tuvalian); and by Cortecci et al. (1981) and Boschetti et al. (2011) for the Norian.

Supplementary data to this article can be found online at https://doi.org/10.1016/j.sedgeo.2022.106104.

Declaration of competing interest

The authors declare no known competing financial interests or personal relationships that could have influenced the work reported in this paper.

Acknowledgements

This study was supported by the following research projects: 2017SGR-824 (SEDIMENTARY GEOLOGY), Departament d'Innovació, Universitats i Empreses of the Catalan Government; CGL2016-79458-P (*Ministerio de Economía y Competitividad*), PGC2018-098272-B-I00, PID2019-104625RB-I00 and PID2020-118999GB-I00 (*Secretaría Estado I+D+I; Ministerio de Ciencia e Innovación*) of the Spanish Government;

and B-RNM-072-UGR18 (FEDER *Andalucía*), P18-RT-4074, and RNM-208 (*Junta de Andalucía*). We thank Laura Rosell (*Universitat de Barcelona*) for help in preparing the isotope tables and interpreting the assemblage of isotope data, Josep Mª Salvany (*Universitat Politècnica de Catalunya*) for supplying samples from the Triassic Catalan basin and help in organize the graphic material, Rosa Marimón and Raúl. Carrey for several years of exhaustive analytical work at the Scientific and Technology Centers of the *Universitat de Barcelona*, Eduard Roca and Frederic Escorsa (*Universitat de Barcelona*) for supplying samples from the Cofrentes outcrop, Eusebio García and Vicent Soriano for help with field work in Valencian areas, editor Catherine Chagué and two anonymous reviewers for significantly improving the manuscript.

References

Alonso-Azcárate, J., Bottrell, S.H., Mas, J.R., 2006. Synsedimentary versus metamorphic control of S, O and Sr isotopic compositions in gypsum evaporites from the Cameros Basin, Spain. Chemical Geology 234, 46–57.

Arche, A., López-Gómez, J., 1996. Origin of the Permian-Triassic Iberian Basin, central-eastern Spain. Tectonophysics 266, 443–464.

Arche, A., López-Gómez, J., 2014. The Carnian Pluvial Event in Western Europe: New data from Iberia and correlation with the Western Neotethys and Eastern North America-NW Africa regions. Earth-Science Reviews 128, 196–231.

Bartrina, T., Hernández, E., 1990. Las unidades evaporíticas del Triásico del subsuelo del Maestrazgo. In: Ortí, F., Salvany, J.M. (Eds.), Formaciones Evaporíticas de la Cuenca del Ebro y Cadenas Periféricas, y de la Zona de Levante. ENRESA-Universitat de Barcelona, Barcelona, pp. 34–38 (in Spanish).

Bernasconi, S.M., Meier, I., Wholwend, S., Brack, P., Hochuli, P.A., Bläsi, H., Wortmann, U.G., Ramseyer, K., 2017. An evaporite-based high-resolution sulfur isotope record of the Late Permian and Triassic seawater sulfate. Geochimica et Cosmochimica Acta 204, 331–349.

Berner, R., 2005. The carbon and sulfur cycles and atmospheric oxygen from middle Permian to middle Triassic. Geochimica et Cosmochimica Acta 69, 3211–3217.

Besems, R.E., 1981a. Aspects of Middle and Late Triassic palynology. 1. Palynostratigraphical data from the Chiclana de Segura Formation of the Linares-Alcaraz region (SE Spain) and correlation with palynological assemblages from the Iberian Peninsula. Review of Palaeobotany and Palynology 32, 257–273.

Besems, R.E., 1981b. Aspects of Middle and Late Triassic palynology. 2. Preliminar palynological data from the Hornos-Siles Formation of the Prebetic zone, NE province of Jaén (SE Spain). Review of Palaeobotany and Palynology 32, 389–400.

Birnbaum, S., Coleman, M., 1979. Source of sulphur in the Ebro Basin (Northern Spain) Tertiary nonmarine evaporite deposits as evidenced by sulphur isotopes. Chemical Geology 25, 163–168.

Boschetti, T., Cortecci, G., Toscani, L., Iacumin, P., 2011. Sulfur and oxygen isotope compositions of the Upper Triassic sulfates from the Northern Apennines (Italy): paleogeograhic and hydrochemical implications. Geologica Acta 9, 129–147.

Brack, P., Rieber, H., Mundil, R., Blendinger, W., Maurer, F., 2007. Geometry and chronology of growth and drowning of Middle Triassic carbonate platforms (Cernera and Biviera/Clapsavon) in the Southern Alps (northern Italy). Swiss Journal of Geosciences 100, 327–347.

Calvet, F., Marzo, M., 1994. El Triásico de las Cordilleras Costero Catalanas: estratigrafía, sedimentología, y análisis secuencial. III Coloquio de Estratigrafía y Paleogeografía del Pérmico y Triásico de España, Cuenca. Excursion guide-book (53 pp.) (in Spanish with English abstract).

Calvet, F., Solé de Porta, N., Salvany, J.M., 1993. Cronoestratigrafía (Palinología) del Triásico sudpirenaico y del Pirineo Vasco-Cantábrico. Acta Geologica Hispánica 28, 33–48 (in Spanish with English abstract).

Carrillo, E., Rosell, L., Ortí, F., 2014. Multiepisodic evaporite sedimentation as an indicator of palaeogeographical evolution in foreland basins (South-eastern Pyrenean basin, Early–Middle Eocene). Sedimentology 61, 2086–2112.

Castillo Herrador, F., 1974. Le Trias évaporitique des basins de la Vallée de l'Èbre et de Cuenca. Bulletin Société Géologique France 16, 666–675 (in French with English abstract).

Claypool, G.E., Holser, W.T., Kaplan, I.R., Sakai, H., Zak, I., 1980. The age curves of sulfur and oxygen isotopes in marine sulfate and their mutual interpretation. Chemical Geology 28, 199–260.

Cortecci, G., Reyes, E., Berti, G., Casati, P., 1981. Sulfur and oxygen isotopes in Italian marine sulfates of Permian and Triassic ages. Chemical Geology 34, 65–79.

Dal Corso, J., Bernardi, M., Sun, Y., Song, H., Seyfullah, L.J., Preto, N., Gianolla, P., Ruffell, A., Kustatscher, E., Roghi, G., Merico, A., Hohn, S., Schmidt, A.R., Marzoli, A., Newton, R.J., Wignall, P.B., Benton, M.J., 2020. Extinction and dawn of the modern world in the Carnian (Late Triassic). Science Advances 6, eaba0099.. https://www.science.org/doi/10.1126/sciadv.aba0099.

De Torres, T., 1990. Primeros resultados de unas dataciones palinológicas del Keuper de la Rama Castellana de la Cordillera Ibérica, Prebético y Subbético frontal. In: Ortí, F., Salvany, J.M. (Eds.), Formaciones Evaporíticas de la Cuenca del Ebro y Cadenas Perféricas, y de la Zona de Levante. ENRESA-Universidad Barcelona, pp. 219–223 (in Spanish).

Doubinger, J., López-Gómez, J., Arche, A., 1990. Pollen and spores from the Permian and Triassic sediments of the southeastern Iberian Ranges, Cueva de Hierro (Cuenca) to Chelva-Manzanera (Valencia-Teruel) region, Spain. Review of Palaeobotany and Palynology 66, 25–45.

Dronkert, H., 1987. Diagenesis of Triassic evaporites in northern Switzerland. Eclogae Geologicae Helvetiae 80, 97–413.

Dronkert, H., Bläsi, H.-R., Matter, A., 1990. Facies and Origin of Triassic Evaporites from the NAGRA Boreholes, Northern Switzerland. Geologische Berichtel, Nr. 12. Landeshydrologie und -geologie, Bern (120 pp.).

Escavy, J.I., Herrero, M.J., Arribas, M.E., 2012. Gypsum resources of Spain: temporal and spatial distribution. Ore Geology Reviews 49, 72–84.

Escudero-Mozo, M.J., Márquez-Aliaga, A., Goy, A., Martín-Chivelet, J., López-Gómez, J., Márquez, L., Arche, A., Plasencia, P., Pla, C., Marzo, M., Sánchez-Fernández, D., 2015. Middle Triassic carbonate platforms in eastern Iberia: evolution of their fauna and palaeogeographic significance in the western Tethys. Palaeogeography, Palaeoclimatology, Palaeoecology 417, 236–260.

Fanlo, I., Ayora, C., 1998. The evolution of the Lorraine evaporite basin: implications for the chemical and isotope composition of the Triassic ocean. Chemical Geology 146, 135–154.

Flinch, J.F., Soto, J.I., 2017. Allochthonous Triassic and salt tectonic processes in the Betic-Rif Orogenic Arc. In: Soto, J.I., Flinch, J.F., Tari, G. (Eds.), Permo-Triassic Salt Provinces of Europe, North Africa and the Atlantic Margins. Elsevier, Amsterdam, pp. 417–446.

Fréchengues, M., Peybernès, B., 1991. Stratigraphie séquentielle du Trias moyen et supérieur des Pyrénées franco-espagnoles. Comptes Rendus Académie Sciences Paris 313, 355–360 (in French with English abstract).

Fréchengues, M., Peybernès, B., Lucas, Cl., Souquet, P., Fournier-Vinas, C., Martini, Zaninetti, L., 1992. Le Trias des Pyrénees Centrales et Orientales Franco-Espagnoles. Livre Guide. Strata, série 217 (90 pp.). (in French).

Furin, S., Preto, N., Rigo, M., Roghi, G., Gianolla, P., Crowley, J.L., Browring, S.A., 2006. High-precision U-Pb zircon age from the Triassic of Italy: implications for the Triassic time scale and the Carnian origin of calcareous nannoplankton and dinosaurs. Geology 34, 1009–1012.

Gaetani, M., Lozowski, V., Szulc, J., Arche, A., Calvet, F., López-Gómez, J., Hirsch, F., 2000. Early Ladinian. In: Decourt, J., Gaetani, M., Vrielynck, B., Barrier, E., Biju-Duval, M.F., Brunet, M.F., Cadet, J.P., Crasquin, S., Sandulesco, M. (Eds.), Peri-Tethys Atlas, Palaeogeographical Maps. Commision for the Geological Map of the World (CCGM/CGMW), Paris, pp. 41–48.

García Veigas, J., Cendón, D.I., Rosell, L., Ortí, F., Torres Ruiz, J., Martín, J.M., Sanz, E., 2013. Salt deposition and brine evolution in the Granada Basin (Late Tortonian, SE Spain). Palaeogeography, Palaeoclimatology, Palaeoecology 369, 452–465.

García-Ávila, M., Mercedes-Martín, R., Juncal, M.A., Diez, J.B., 2020. New palynological data in Muschelkalk facies of the Catalan Coastal Ranges (NE of the Iberian Peninsula). Comptes Rendus Géoscience 352, 443–454.

Geisler, D., Adloff, M.C., Doubinger, J., 1978. Découverte d'une microflore du Carnien inférieur dans la série salifère de Lorraine. Sciences de la Terre 22, 391–399 (in French with English abstract).

Gibbons, W., Moreno, M.T. (Eds.), 2002. The Geology of Spain. Geological Society, London (649 pp.).

Gibert, L., Ortí, F., Rosell, L., 2007. Plio-Pleistocene lacustrine evaporites of the Baza Basin (Betic Chain, SE Spain). Sedimentary Geology 200, 89–116.

Gómez, J.J., Goy, A., 1998. Las unidades litoestratigráficas del tránsito Triásico-Jurásico en la región de Lécera (Zaragoza). Geogaceta 23, 63–66 (in Spanish with English abstract).

Gómez, J.J., Castaño, S., Sanz, D., 2004. Origen geológico de los contaminantes (sulfatos) presentes en las aguas subterráneas de la Laguna de Pétrola (Albacete, España). Resultados preliminares. Geogaceta 35, 167–170 (in Spanish with English abstract).

Gómez, J.J., Goy, A., Barrón, E., 2007. Events around the Triassic-Jurassic boundary in northern and eastern Spain: a review. Palaeogeography, Palaeoclimatology, Palaeoecology 244, 89–110.

Gordon, W.A., 1975. Distribution by latitude of Phanerozoic evaporite deposits. Journal of Geology 83, 671–684.

Götzinger, M.A., Lein, R., Pak, E., 2001. Geologie, Mineralogie und Schwefelisotopie ostalpiner "Keuper-Gipse": Vorbericht und Diskussion. Mitteilungen der Österreichische Mineralogische Gesellschaft 146, 95–96.

Gündoğan, İ., Helvaci, C., Sözbilir, H., 2008. Gypsiferous carbonates at Honaz Dağı (Denizli): first documentation of Triassic gypsum in western Turkey and its tectonic significance. Journal of Asian Earth Sciences 32, 49–65.

Hardie, L.A., 1967. The gypsum-anhydrite equilibrium at one atmosphere pressure. American Mineralogist 52, 171–200.

He, T., Dal Corso, J., Newton, R.J., Wignall, P.B., Mills, B.J.W., Todaro, S., Di Stefan, P., Turner, E.C., Robert, A., Jamieson, R.A., Randazzo, V., Rigo, M., Jones, R.E., Dunhill, A.M., 2020. An enormous sulfur isotope excursion indicates marine anoxia during the end-Triassic mass extinction. Science Advances 6, eabb6704.. https://www.science.org/doi/10.1126/sciadv.abb6704.

Hernando, S., 1977. Pérmico y Triásico de la Región Ayllón-Atienza. (Ph.D. thesis) Seminarios de Estratigrafía. Series MonográficaVol 2. Dpt. Estratigrafía, Universidad Complutense de Madrid (408 pp.). (in Spanish).

Holser, W.T., 1977. Catastrophic chemical events in the history of the ocean. Nature 267, 403–408.

Holser, W.T., Kaplan, I.R., 1966. Isotope geochemistry of sedimentary sulfates. Chemical Geology 1, 93–135.

Holser, W.T., Clemente, G.P., Jansa, L.F., Wade, J.A., 1988. Evaporite deposits of the North Atlanic Rift. In: Manspeizer, W. (Ed.), Triassic-Jurassic Rifting; Continental Breakup and the Origin of the Atlantic Ocean and Passive Margins. Developments in Geotectonics Parts A and B. Elsevier, Amsterdam, pp. 525–556.

Horacek, M., Brandner, R., Richoz, S., Povoden-Karadeniz, E., 2010. Lower Triassic sulphur isotope curve of marine sulphates from the Dolomites, N-Italy. Palaeogeography, Palaeoclimatology, Palaeoecology 290, 65–70.

Insalaco, E., Virgone, A., Courme, B., Gaillot, J., Kamali, M., Moallemi, A., Lotfpour, M., Monibi, S., 2006. Upper Dalan Member and Kangan Formation between the Zagros

Mountains and offshore fars, Iran: depositional system, biostratigraphy and stratigraphic architecture. GeoArabia 11, 75–176.
Iribar, V., Ábalos, B., 2011. The geochemical and isotopic record of evaporite recycling in spas and salterns of the Basque Cantabrian basin, Spain. Applied Geochemistry 26, 1315–1329.
Jurado, M.J., 1989. El Triásico del Subsuelo de la Cuenca del Ebro. Ph.D. thesisUniversidad de Barcelona (259 pp. in Spanish).
Jurado, M.J., 1990. El Triásico y el Liásico basal evaporíticos del subsuelo de la cuenca del Ebro. In: Ortí, F., Salvany, J.M. (Eds.), Formaciones Evaporíticas de la Cuenca del Ebro y Cadenas Periféricas, y de la Zona de Levante. ENRESA-Universidad de Barcelona, pp. 54–58 (in Spanish).
Kampschulte, A., Strauss, H., 2004. The sulphur isotopic evolution of Phanerozoic seawater based on the analysis of structural substituted sulphate in carbonates. Chemical Geology 204, 255–286.
Kampschulte, A., Buhl, D., Strauss, H., 1998. The sulfur and strontium isotope compositions of Permian evaporites from the Zechstein basin, northern Germany. Geologische Rundschau 87, 192–199.
Klimowitz, J., Malagón, J., Quesada, S., Serrano, A., 1999. Desarrollo y evolución de estructuras salinas mesozoicas en la parte suroccidental de la Cuenca Vasco-Cantábrica (Norte de España): implicaciones exploratorias. In: AGGEP (Ed.), Libro Homenaje a José Ramírez del Pozo. Asociación de Geologos y Geofísicos Españoles del Petróleo, Madrid, pp. 159–166 (in Spanish).
Lindh, T.B., 1983. Temporal Variations in ^{13}C, ^{34}S and Global Sedimentation During the Phanerozoic. (M.Sc. thesis)University of Miami (98 pp.).
Lloyd, R.M., 1968. Oxygen isotope behaviour in the sulfate-water system. Journal of Geophysical Research 73, 6099–7110.
Longinelli, A., Flora, O., 2007. Isotopic composition of gypsum samples of Permian and Triassic age from the north-eastern Italian Alps: palaeoenvironmental implications. Chemical Geology 245, 275–284.
López-Gómez, J., Arche, A., Calvet, F., Goy, A., 1998. Epicontinental marine carbonate sediments of the Middle and Upper Triassic in the westernmost part of the Tethys Sea, Iberian Peninsula. Zentralblatt für Geologie und Paläontologie 1, 1033–1084.
Martín-Algarra, A., Vera, J.A., 2004. La Cordillera Bética y las Baleares en el contexto del Mediterráneo Occidental. In: Vera, J.A. (Ed.), Geología de España. SGE-769 IGME, Madrid, pp. 352–354 (in Spanish).
Martínez del Olmo, W., Motes, K., Martín, D., 2015. El papel del diapirismo de la sal triásica en la estructuración del Prebético (SE de España). Revista de la Sociedad Geológica de España 28, 3–24 (in Spanish with English abstract).
Mietto, P., Manfrin, S., Preto, N., Rigo, M., Roghi, G., Furin, S., Gianolla, P., Posenato, R., Muttoni, G., Nicora, A., Buratti, N., Cirilli, S., Spötl, C., Ramezani, J., Bowring, S.A., 2012. The Global Boundary Stratotype Section and Point (GSSP) of the Carnian Stage (Late Triassic) at Prati di Stuores/Stoures Wiesen Section (Southern Alps, NE Italy). Episodes 35, 414–430.
Morad, S., Al-Aasm, I.S., Longstaffe, F.J., Marfil, R., De Ros, L.F., Johansen, H., Marzo, M., 1995. Diagenesis of a mixed siliciclastic/evaporitic sequence of the Middle Muschelkalk (Middle Triassic), the Catalan Coastal Ranges, NE Spain. Sedimentoloy 42, 749–768.
Mossop, D.G., Shearman, D.J., 1973. Origin of secondary gypsum rocks. Transactions of the Institution of Mining and Metallurgy, Section B Applied Earth Science82 pp. 147–154.
Mundil, R., Palfy, J., Renne, P.R., Brack, P., 2010. The Triassic timescale: new constraints and a review of geochronological data. Triassic Timescale334 pp. 41–60.
Murray, R.C., 1964. Origin and diagenesis of gypsum and anhydrite. Journal Sedimentary Petrology 34, 512–523.
Nebot, M., Guimerà, J., 2016. Kinematic evolution of a fold-and-thrust belt developed during basin inversion: the Mesozoic Maestrat basin, E Iberian Chain. Geological Magazine 155, 630–640.
Newton, R.J., Pevitt, E.L., Wignall, P.B., Bottrell, S.H., 2004. Large shifts in the isotopic composition of seawater sulphate across the Permo-Triassic boundary in northern Italy. Earth and Planetary Science Letters 218, 331–345.
Ortí, F., 1974. El Keuper del Levante español. Estudios Geológicos 30, 7–46 (in Spanish with English abstract).
Ortí, F., Pérez-López, A., García-Veigas, J., Rosell, L., Cendón, D.I., Pérez-Valera, F., 2014. Sulfate isotope compositions ($\delta^{34}S$, $\delta^{18}O$) and strontium isotopic ratios ($^{87}Sr/^{86}Sr$) of Triassic evaporites in the Betic Cordillera (SE Spain). Revista de la Sociedad Geológica de España 27, 79–89 (in Spanish with English abstract).
Ortí, F., Pérez-López, A., Salvany, J.M., 2017. Triassic evaporites of Iberia: Sedimentological and palaeogeograpical implications for the western Neotethys evolution during the Middle Triassic-Earliest Jurassic. Palaeogeography, Palaeoclimatology, Palaeoecology 471, 157–180.
Ortí, F., Salvany, J.M., Rosell, L., Castelltort, X., Inglès, M., Playà, E., 2018. Middle Triassic evaporite sedimentation in the Catalan basin: implications for the palaeogeographic evolution in the NE Iberian platform. Sedimentary Geology 374, 158–178.
Ortí, F., Guimerà, J., Götz, A., 2020. Middle-Upper Triassic stratigraphy and structure of the Alt Palància (eastern Iberian Chain): a multidisciplinary approach. Geologica Acta 18 (4), 1–25.
Ortí, F., Guimerà, J., Benedicto, C., Pérez-López, A., 2021. Middle-Upper Triassic successions in the eastern Iberian Chain (Alt Palància and Manzanera areas): stratigraphic precisions. Geo-Temas 18, 174–177.
Pearson, F.J., Balderer, W., Loosli, H.H., Lehaman, B.E., Matter, A., Peters, Tj, Schmassmann, H., Gautschi, A., 1991. Applied Isotope Hydrogeology - A Case Study in Northern Switzerland. Studies in Environmental Science43. Elsevier, Amsterdam (460 pp.).
Pérez-López, A., 1996. Sequence model for coastal-plain depositional systems of the Upper Triassic (Betic Cordillera, southern Spain). Sedimentary Geology 101, 99–117.
Pérez-López, A., 1998. Epicontinental Triassic of the Southern Iberian Continental Margin (Betic Cordillera, Spain). In: Bachmann, G.H., Lerche, I. (Eds.), Epicontinental Triassic. Zentralblatt für Geologie und Paläontologie1, pp. 1009–1031.
Pérez-López, A., Pérez-Valera, F., 2007. Palaeogeography, facies and nomenclature of the Triassic units in the different domains of the Betic Cordillera (S Spain). Palaeogeography, Palaeoclimatology, Palaeoecology 254, 606–626.
Pérez-López, A., Fernández, J., Solé de Porta, N., Márquez, Aliaga A., 1991. Bioestratigrafía del Triásico de la Zona Subbética (Cordillera Bética). Revista Espanola de Paleontologia 139–150 (N. Extraor). (in Spanish with English abstract).
Pérez-López, A., Solé de Porta, N., Ortí, F., 1996. Facies carbonato-evaporíticas del Trías Superior y tránsito al Lías en el Levante español: nuevas precisiones estratigráficas. Cuadernos Geología Ibérica 20, 245–269 (in Spanish with English abstract).
Pérez-López, A., Pérez-Valera, F., Götz, A.E., 2012. Record of epicontinental platform evolution and volcanic activity during a major rifting phase: the Late Triassic Zamoranos Formation (Betic Cordillera, S Spain). Sedimentary Geology 247-248, 39–57.
Pérez-López, A., Benedicto, C., Ortí, F., 2021a. Middle Triassic carbonates of Eastern Iberia (Western Tethyan Realm): a shallow platform model. Sedimentary Geology 420, 105904. https://doi.org/10.1016/j.sedgeo.2021.105904.
Pérez-López, A., Cambeses, A., Pérez-Valera, F., Götz, A.E., 2021b. Rhaetian tectonomagmatic evolution of the Central Atlantic Magmatic Province volcanism in the Betic Cordillera, South Iberia. Lithos 369-397, 106230. https://doi.org/10.1016/j.lithos.2021.106230.
Playà, E., Ortí, F., Rosell, L., 2000. Marine to non-marine sedimentation in the upper Miocene evaporites of the Eastern Betics, SE Spain: sedimentological and geochemical evidence. Sedimentary Geology 133, 135–166.
Preto, N., Kustatscher, E., Wignall, P.B., 2010. Triassic climates - state of the art and perspectives. Palaeogeography, Palaeoclimatology, Palaeoecology 290, 1–10.
Prokoph, A., Shields, G.A., Veizer, J., 2008. Compilation and time-series analysis of a marine carbonate $\delta^{18}O$, $\delta^{13}C$, $^{87}Sr/^{86}Sr$ and $\delta^{34}S$ database through Earth history. Earth-Science Reviews 87, 113–133.
Raab, M., Spiro, B., 1991. Sulfur isotopic variations during seawater evaporation with fractional crystallization. Chemical Geology 86, 323–333.
Rick, B., 1990. Sulphur and oxygen isotopic composition of Swiss Gipskeuper (Upper Triassic). Chemical Geology, Isotope Geoscience Section 80, 243–250.
Rossi, C., Vilas, L., Arias, C., 2015. The Messinian marine to nonmarine gypsums of Jumilla (Northern Betic Cordillera, SE Spain): isotopic and Sr concentration constraints on the origin of parent brines. Sedimentary Geology 328, 96–114.
Rouchy, J.M., Pierre, C., 1979. Données sédimentologiques et isotopiques sur les gypses des séries évaporitiques messiniennes d'Espagne méridionale et the Chypre. Revue de Géologie Dynamique et de Géographie Physique 21, 267–280.
Salvany, J.M., Bastida, J., 2004. Análisis litoestratigráfico del Keuper surpirenaico central. Revista de la Sociedad Geológica de España 17, 3–26 (in Spanish with English abstract).
Salvany, J.M., Ortí, F., 1987. El Keuper de los Catalánides. Cuadernos Geología Ibérica 11, 215–236 (in Spanish with English abstract).
Schobben, M., Stebbins, A., Ghaderi, A., Strauss, H., Korn, D., Korte, C., 2015. Flourishing ocean drives the end-Permian marine mass extinction. Proceedings of the National Academy of Sciences of the United States of America 112, 10298–10303.
Schroll, E., Rantitsch, G., 2005. Sulfur isotope patterns in the Bleiberg deposit (Eastern Alps) and their implications for genetically affiliated. Mineralogy and Petrology 84, 1–18.
Schroll, E., Shulz, O., Pak, E., 1983. Sulphur isotope distribution in the Pb-Zn deposit Bleiberg (Carinthia, Austria). Mineralium Deposita 18, 17–25.
Scotese, Ch.R., Song, H., Mills, B.J.W., Van der Meer, D.G., 2021. Phanerozoic paleotemperatures: the earth's changing climate during the last 540 million years. Earth-Science Reviews 215, 103503.
Solé de Porta, N., Ortí, F., 1982. Primeros datos cronoestratigráficos de las series evaporíticas del Triásico superior de Valencia. Acta Geologica Hispánica 17, 185–191 (in Spanish with English abstract).
Solé de Porta, N., Calvet, F., Torrentó, L., 1987. Análisis palinológico del Triásico de los Catalánides (NE España). Cuadernos Geología Ibérica 11, 237–254 (in Spanish with English abstract).
Song, H., Tong, J., Algeo, T.J., Song, H., Qiu, H., Zhu, Y., Tian, L., Bates, S., Lyons, T.W., Luo, G., Kump, L.R., 2014. Early Triassic seawater sulfate drawdown. Geochimia et Cosmochimica Acta 128, 95–113.
Sopeña, A., López-Gómez, J., Arche, A., Pérez-Arlucea, M., Ramos, A., Virgili, C., Hernando, S., 1988. Permian and Triassic basins of the Iberian península. In: Manspeizer, W. (Ed.), Triassic-Jurassic Rifting. Continenal Breakup and the Origin of the Atlantic Ocean and Passive Margins, Part B22. Developments in Geotectonics, pp. 758–785.
Soto, J.I., Flinch, J.F., Tari, G., 2017. Permo-Triassic basins and tectonics in Europe, North Africa and the Atlantic Margins: a Synthesis. In: Soto, J.I., Flinch, J.F., Tari, G. (Eds.), Permo-Triassic Salt Provinces of Europe, North Africa and the Atlantic Margins. Tectonic and Hydrocabon Potential. Elsevier, Amsterdam, pp. 3–41.
Spölt, C., 1988. Zur Altersstelung permoskythischer Gipse im Raum des östlichen Karwendelgebirges (Tirol). Geologisch-Paläontologische Mitteilungen Innsbruck 14, 197–212 (in German with English abstract).
Spötl, C., Pak, E., 1996. A strontium and sulfur isotope study of Permo-Triassic evaporites in the Northern Calcareous Alps, Austria. Chemical Geology 131, 219–234.
Stefani, M., Furin, S., Gianolla, P., 2010. The changing climate framework and depositional dynamics of Triassic carbonate platforms from the Dolomites. Palaeogeography, Palaeoclimology, Palaeoecology 290, 43–57.
Strauss, H., 1997. The isotopic composition of sedimentary sulfur through time. Palaeogeography, Palaeoclimatology, Palaeoecology 132, 97–118.
Sun, Y., Joachimski, M.M., Wignall, P.B., Yan, C., Chen, Y., Jiang, H., Wang, L., Lai, X., 2012. Lethally hot temperatures during the Early Triassic Greenhouse. Science 338, 366–370.
Thierry, J., 2000. Late Sinemurian. In: Decourt, J., Gaetani, M., Vrielynck, B., Barrier, E., Biju-Duval, M.F., Brunet, M.F., Cadet, J.P., Crasquin, S., Sandulescu, M. (Eds.), Peri-Tethys

Atlas, Palaeogeographical Maps. Commision for the Geological Map of the World (CGM/CGMW), Paris, pp. 49–59.
Thode, H.G., Monster, J., 1965. Sulfur isotope geochemistry of petroleum, evaporites and ancient seas. American Association Petroleum Geologists Memoir4 pp. 367–377.
Utrilla, R., Pierre, C., Ortí, F., Pueyo, J.J., 1992. Oxygen and sulfur isotope composition as indicators of the origin of the Mesozoic and Cenozoic evaporites from Spain. Chemical Geology 102, 229–244.
Vera, J.A. (Ed.), 2004. Geología de España. Sociedad Geológica España-Instituto Geológico Minero España, Madrid (890 pp.) (in Spanish).
Virgili, C., Sopeña, A., Ramos, A., Hernando, S., 1977. Problemas de la cronoestratigrafía del Trías en España. Cuadernos Geología Ibérica 4, 57–88 (in Spanish with English abstract).
Warren, J.K., 2006. Evaporites: Sediments, Resources, Hydrocarbons. Springer-Verlag, Berlin Heidelberg (1035 pp.).
Williford, K.H., Foriel, J., Ward, P.D., Steig, E.J., 2009. Major perturbation in sulfur cycling at the Triassic-Jurassic boundary. Geology 37, 835–838.
Worden, R.H., Smalley, P.C., Fallick, A.E., 1997. Sulfur cycle in buried evaporites. Geology 25, 643–646.
Wotzlaw, J.F., Guex, J., Bartolini, A., Gallet, Y., Krystyn, L., McRoberts, C.A., Taylor, D., Schoene, B., Schaltegger, U., 2014. Towards accurate numerical calibration of the Late Triassic: high precision U-Pb geochronology constraints on the duration of the Rhaetian. Geology 42, 571–574.
Ziegler, P.A., 1982. Triassic rifts and facies patterns in Western and Central Europe. Geologische Rundschau 71, 747–772.
Ziegler, P.A., 1988. Post-Hercynian plate reorganization in the Tethys and Artic-North Atlantic domains. In: Manspeizer, W. (Ed.), Triassic-Jurassic Rifting. Continental Breakup and the Origin of the Atlantic Ocean and Passive Margins. Developments in Geotectonics 22B. Elsevier, Amsterdam, pp. 711–755.